Received: 3 July 2020 | Revised: 21 October 2020 | Accepted: 31 January 2021

DOI: 10.1002/mmce.22589

REVIEW ARTICLE

INTERNATIONAL JOURNAL OF RF AND MICROWAVE COMPUTER-AIDED ENGINEERING WILEY

A chronological review of circularly polarized dielectric resonator antenna: Design and developments

Priya Ranjan Meher[1] | **Bikash Ranjan Behera**[1] | **Sanjeev Kumar Mishra**[1] | **Ayman Abdulhadi Althuwayb**[2]

[1]Department of Electronics and Telecommunication Engineering, International Institute of Information Technology, Bhubaneswar, India

[2]Department of Electrical Engineering, Jouf University, Sakaka, Saudi Arabia

Correspondence
Sanjeev Kumar Mishra, Department of Electronics and Telecommunication Engineering, International Institute of Information Technology, Bhubaneswar, India.
Email: sanjeev@iiit-bh.ac.in

Abstract

This article presents a chronological overview of circularly polarized dielectric resonator antennas (CPDRAs). This article provides a comprehensive review about innovation and rapid developments of CPDRAs over the last three and half decades since 1986s. The objective of this article is to highlight the basic concept of CP mechanism in DRA and state-of-the-art developments of CPDRAs in terms of single and multi-point feed for unmodified and modified DR geometries considering different types of excitation mechanism such as microstrip line, coaxial probe, and aperture coupled feed. To give insights into circular polarization, Authors proposed a compact modified CPDRA. It offers simulated bandwidth of 47.5% (2.34-3.80 GHz), measured impedance bandwidth of 50.8% (2.26-3.78), and simulated axial bandwidth of 13% (3.29-3.75 GHz) respectively. Other antenna parameters such as peak realized gain and radiation efficiency are 7.7 dBi and 98% within operating frequency bands, respectively. The proposed outcomes confirm that the proposed CPDRA can be used as a suitable candidate for wireless body area network applications.

KEYWORDS

broadband, circular polarization (CP), dielectric resonator antenna (DRA), feeding mechanism, modified DR shape

1 | INTRODUCTION

In the present scenario, wideband characteristics and low profile antennas are essential for modern wireless communication systems. To meet the above requirements, DRA is an emerging solution. It possesses numerous advantages such as high efficiency, low metallic loss, minimum surface waves, wideband characteristics, and degree of design freedom.[1-7] DRA consists of a dielectric resonator (DR) that is made of a non-conducting material, a ground plane, and a dielectric substrate resides in between the DR and the ground plane. The resonant frequency of DRA depends on the permittivity and physical size of three dimensional DRs like radius for hemispherical shape, height-to-radius ratio for cylindrical shape, and depth-to-width as well as length-to-width ratio for rectangular shape. Figure 1 shows different shapes of DR. The research on DR begun long back in the era of 1930s, where in 1939, it was conceptualized by Richtmger,[8] showing DR as a high Q-factor non-conducting material, but it was used as an effective electromagnetic radiator in 1983. Initially, Long, et al[9] have introduced cylindrical dielectric cavity antenna, consisting of leaky waveguide model (magnetic conductor model) of the dielectric substrate. Since then, it has grown up rapidly with

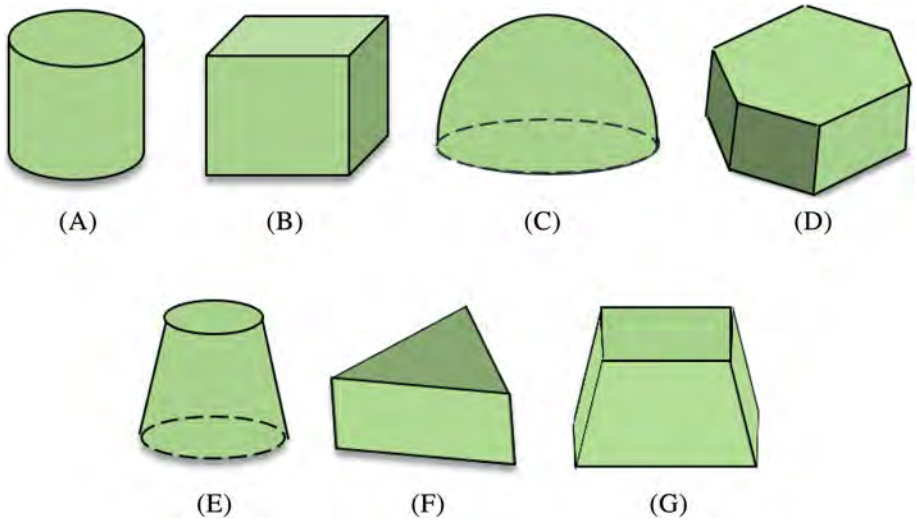

FIGURE 1 Different shapes of dielectric resonator antenna (A) Cylindrical, (B) Rectangular, (C) Hemispherical, (D) Hexagonal, (E) Conical, (F) Triangular, (G) Trapezoidal

implementation of various techniques to enhance the performance of the DRA.

In the current era of communication, CPDRA plays a vital role in modern wireless communication because of its several striking characteristics such as independent of antenna orientation between transmitter and receiver, high reflectivity, high absorption, improved weather penetration, and very less multipath distortion as compared to linearly polarized (LP) antennas. Due to these attractive features, the CP antenna is widely used in various communication like satellite communication systems, mobile communication systems, navigation systems and radar systems. On analyzing the open literature survey, few review articles are available on DRAs. The review article[1] only discussed excited modes and the radiation characteristics of DRAs of different shapes such as cylindrical, cylindrical ring, spherical, and rectangular. In addition, accurate closed form expressions are derived for calculating the resonance frequency, radiation Q-factor, and the inside field of cylindrical DR. Similarly, review article[2] has highlighted types of operating frequency bands that is, broadband, ultra-wideband (UWB) and multiband without considering the circular polarization. Consequently, the review articles[3-7] only considered the selected CPDRAs structure which is considered in this review paper. In view of these, the research on chronological developments of CPDRAs of single and multipoint feed for both unmodified and modified structures considering all excitation approaches such as microstrip line, aperture coupled, and coaxial probe feeding from starting date to now is quite essential for upcoming researchers. To mitigate these points, this review article presents a comprehensive review of CPDRAs based on the abovementioned crucial points. In this review article, the authors have demonstrated a chronological overview of CPDRA over last three and half decades. In addition, the authors have proposed a compact modified rectangular DRA to generate CP radiation waves. The utilization of various CP techniques is essential from research point of view, but cognitively it is incomplete without practical field of potential applications. By considering such scenarios, authors have reported the potential applications in terms of frequency band from the instances available in open literature on CPDRA. The outline of the review article is shown in Figure 2.

To the best of authors' knowledge, this review article is covering all the developing techniques and mechanisms dedicated to generating CP radiation fields. This type of review article seems to be equally important among the antenna designers and researchers working on field of CPDRA. The overall study is segregated as follows: Basic of CP mechanism correlated with DRA is illustrated in Section 2. A state-of-the-art towards generating of CP radiation fields using different techniques such as feeding technique with unmodified and modified DR shapes along with excitation of microstrip line, coaxial probe and aperture coupled feed are reported in Section 3. Proposed structure is briefly explored in Section 4. Potential applications of the open literature survey papers on CPDRAs are also reported in Section 5, followed by conclusion in Section 6.

2 | BASIC OF CP MECHANISM FOR DRA

In this section, the basic concept involved in CP mechanism for the case of DRA is highlighted. Polarization describes the orientation of electric field vectors with respect to time at a particular point in free space. It also can be defined as the wave transmitted or received by an antenna in a given direction.[10] Polarization is categorized into linear polarization (LP) either horizontal or vertical, elliptical polarization (EP) and circular polarization (CP).

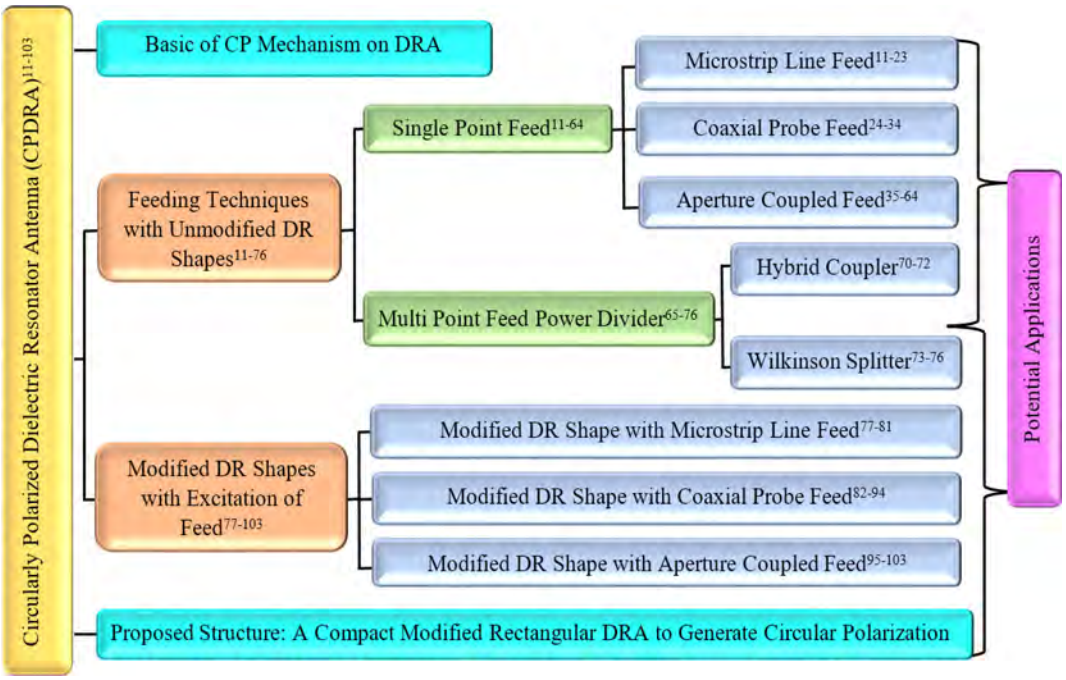

FIGURE 2 The outlines of the review article on circularly polarized CPDRA

In CP waves, both electric field components are equal in magnitude with 90° phase difference. The electric field of two components x and y as a function of time along with positive z-direction of propagation can be written as[10]:

$$E(z,t) = \left(E_{xo}e^{j\omega t}\hat{x} + E_{yo}e^{j\omega t}\hat{y}\right)e^{-j\beta z} \quad (1)$$

where, $E_{xo}e^{j\omega t}\hat{x}$and $E_{yo}e^{j\omega t}\hat{y}$ are x- and y-component of E-field. By solving the above equation and considering the physically realizable part, we get:

$$E(z,t) = E_{xo}\cos(\omega t - \beta z)\hat{x} + E_{yo}\cos(\omega t - \beta z)\hat{y} \quad (2)$$

For CP, $E_{xo} = E_{yo} = E_o$ (equal magnitude), $E_{xo} = E_o e^{jo}$ and $E_{yo} = E_o e^{j\frac{\pi}{2}}$ (orthogonal phase).

By applying the CP conditions, the resultant equation will be:

$$E(z,t) = E_o\cos(\omega t - \beta z)\hat{x} + E_o e^{j\frac{\pi}{2}}\cos(\omega t - \beta z)\hat{y} \quad (3)$$

At a fixed position that is, $z = 0$ (direction of propagation), the Equation (3) can be written as:

$$E(0,t) = E_o\cos(\omega t)\hat{x} + E_o\cos\left(\omega t + \frac{\pi}{2}\right)\hat{y} \quad (4)$$

By applying the different phases that is, $\omega t = 0°$, 90°, 180°, and 270° in Equation (4), the corresponding graphical representation of x and y component of electric fields

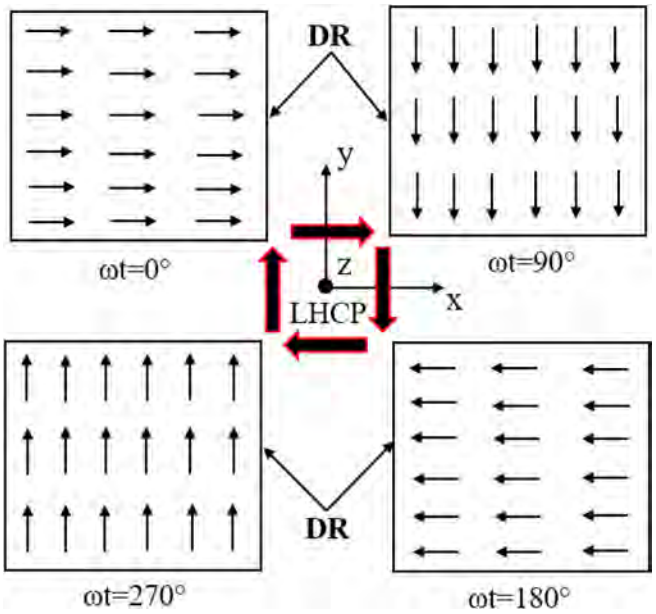

FIGURE 3 Electric field distribution inside the rectangular DRA at different phases

are shown in Figure 3. The phase shifted from 0° to 90°, and the movement of electric field inside the DR is also shifted from right side (+ve) to down side (−ve) of the DR, which confirm the formation of orthogonal modes in DR. Hence, it leads to achievement of CP radiation fields.

For four different phases, the rotation of electric field is in a clockwise motion with respect to the direction of propagation as it can be seen Figure 3. Thus, it confirmed

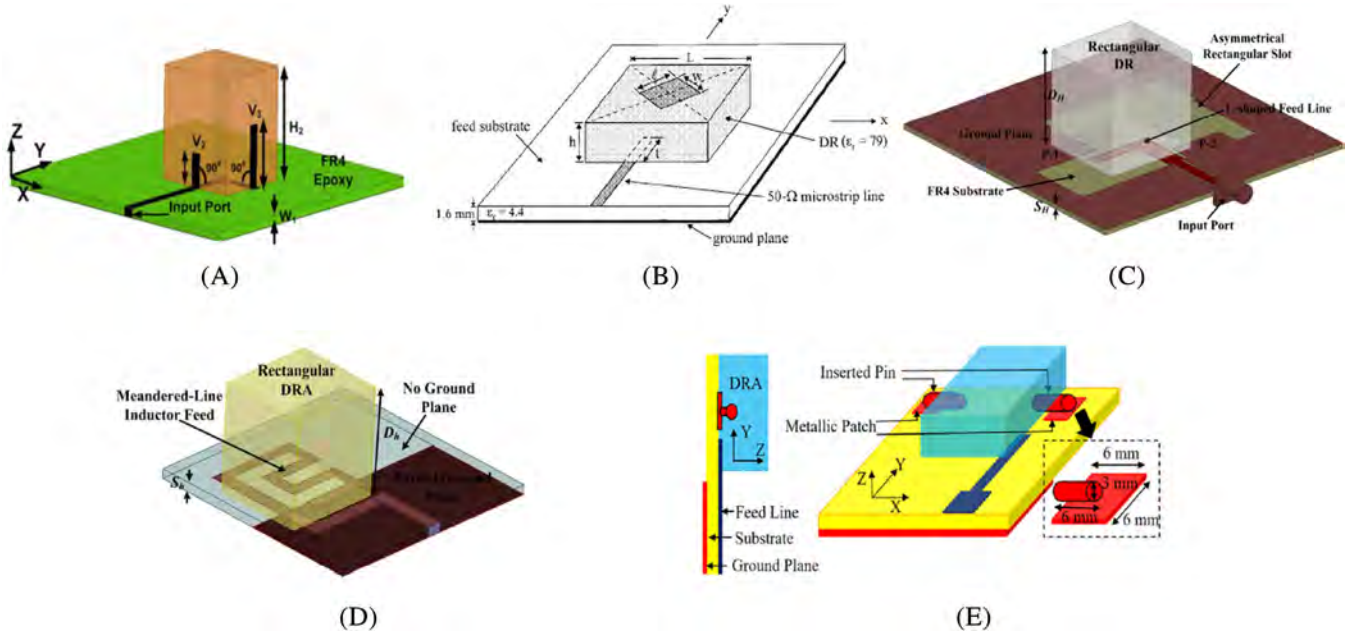

FIGURE 4 Different microstrip feeding structure approaches for circular polarization (A) Dual metallic strips,[12] (B) Metallic loading,[13] (C) Slot on ground plane,[16] (D) Meandered-line,[19] (E) Edge feed with Glueless tech[23]

left-handed circular polarization (LHCP) radiation fields. In the next section, a detailed analogy is drawn in pursuit of different techniques that are used to generate CP for the case of DRA.

3 | TECHNIQUES TO GENERATE CPDRA

This section highlights the state-of-the-art developments of CPDRA using single point feed[11-64] and multi-point feed power divider,[65-76] along with modification of three dimensional DR shapes.[77-103] In this review article, the authors have segregated CP mechanism in terms of excitation of feeding techniques like microstrip line, coaxial probe, and aperture coupled feed, which will be helpful to the researcher to get the complete idea about the developments of particular excitation feeding method.[11-103]

3.1 | Feeding techniques with unmodified DR

One of the fundamental subjects in the broad area of DRA is the excitation scheme, which deals with the problem of how to couple the electromagnetic energy from the feeding transmission line to the dielectric radiator efficiently. Feeding techniques can be divided into single point feed and multi-point feed power divider, which plays an important role in generation of CP for the case of DRA over three and half decades.[11-76]

3.1.1 | Single point feed

DRA is able to radiate electromagnetic energy into free space by excitation of single feeding technique. In this excitation, the generation of CP is obtained due to excitation of two orthogonal modes within the DR structure which are in 90° phase difference with equal magnitude. For better understanding the different excitation, it is segregated into three types of excitation methods that is, microstrip line feed, coaxial probe feed, and aperture coupled feed.[11-64]

Microstrip line feed

The research on CPDRA using single microstrip line feed started with configurations on dual metallic strips around the DR that are not connected with the feed line[11] to generate orthogonal modes resulting in CP radiation fields. Similarly, dual vertical metallic strips around the DR walls[12] which are connected with microstrip feed line to generate CP radiation fields. Consequently, single feed with metallic loading on the surface of DR[13,14] to generate CP response. Others techniques based on slot in the ground plane such as microstrip feed with two pair unequal slots on the infinite ground plane[15] and L-shaped with modified rectangular slot[16] have been investigated for CP characteristics. However, the fabrication

TABLE 1 Outcomes of excitation of microstrip line feed with unmodified DRAs[11-23]

References	DR Shape	$\epsilon_{r,dr}$	Imp BW (GHz)	AR BW (GHz)	G (dB)	η (%)	Modes	CP mechanism
11	Cyli.	9.5	~5.5-6.9	~6.25-6.37	3.2	NM	NM	Metallic strips
12	Rect.	9.8	3.48-5.05	3.67-4.24	6.4	NM	$TE^{x}_{\delta 11}, TE^{y}_{1\delta 1}, TE^{x}_{\delta 13}, TE^{y}_{1\delta 3}$	Metallic strips
13	Squa.	79	~2.2-2.3	2.20-2.24	3.3	NM	TE_{111}	Metallic loading
14	Cyli.	20.8	2.65-3.13	2.84-2.94	NA	NM	NM	Metallic loading
15	Cyli.	79	~2.25-2.43	~2.24-2.29	5.9	NM	NM	Slot on ground
16	Rect	9.8	1.87-4.39	1.75-2.73	3.6	95	$TE^{x}_{\delta 11}, TE^{y}_{1\delta 1}$	Slot on ground
17	Cyli.	38	4.07-4.36	4.18-4.23	5.5	NM	NM	Y-shaped feed
18	H. Cyli.	10.2	4.5-11.8	5.4-7.65	~4.1	NM	$TM_{01\delta} HEM_{11\delta}$	Monopole
19	Rect.	9.8	2.39-2.94	2.19-2.90	2.75	76.86	$TE_{11\delta}$	Meandered-line
20	Rect.	9.8	2-4	2.1-3.4	2.3	NM	$TE^{x}_{111}, TE^{y}_{111}$	Flag-shaped
21	Squa.	9.8	1.8-4	2.5-3.9	1.8	93	$TE^{x}_{111}, TE^{y}_{111}$	Truncated patch
22	Cyli	9.8	3.66-10.35	4.31-7.53 8.84-9.35	5.0	97	—	Edge feed
23	Rect.	9.8	5.59-11.6	5.82-9.41	4.6	93.9	—	Edge feed with Glueless tech.

Note: "~": estimated from graph; AR BW, axial ratio bandwidth; Cyli., cylindrical; G, gain; H. Cyli., half cylindrical; Imp BW, impedance bandwidth; NM, not mentioned; Rect., rectangular; Squa., square; Tech., technique; $\epsilon_{r,dr}$, dielectric constant of DR; η, efficiency.

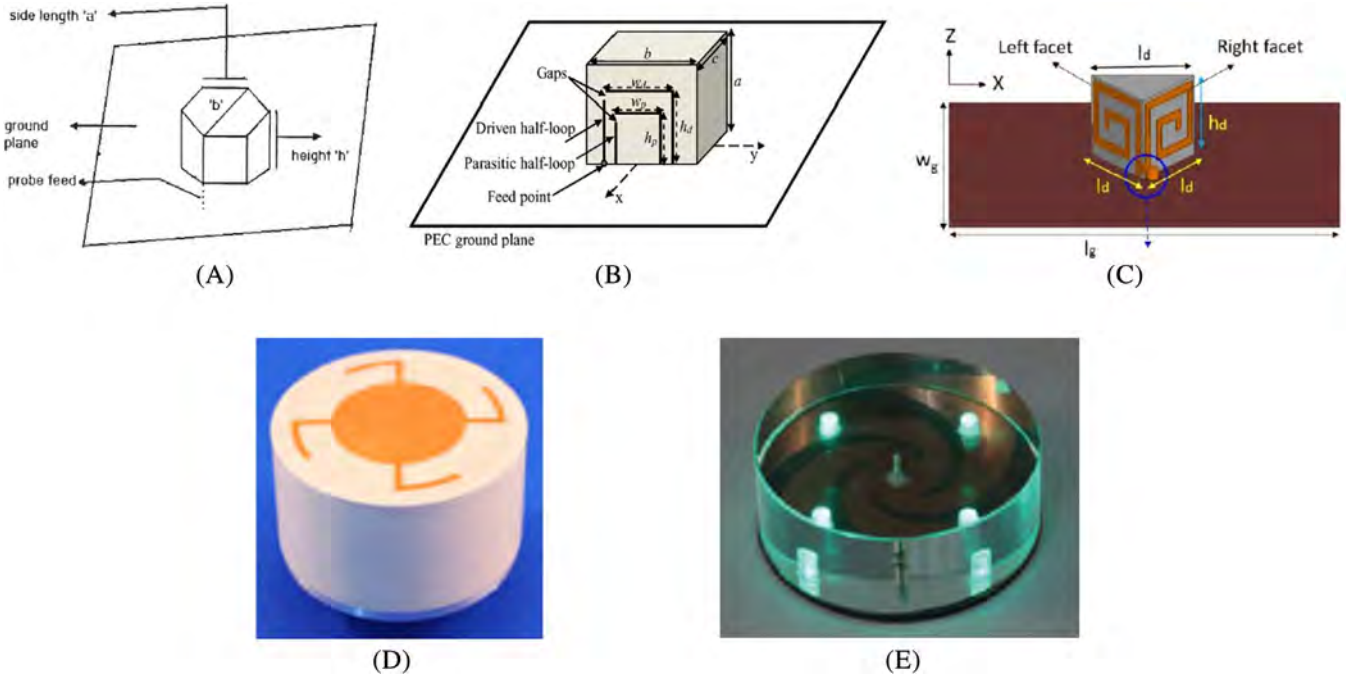

FIGURE 5 Different coaxial probe feeding structure approaches for circular polarization (A) Pentagonal DR with feed,[25] (B) Metallic strips,[27] (C) Dual facet spiral loop,[29] (D) Modified Alford loop,[32] (E) Logarithmic spiral slots[33]

process of the above techniques may be difficult due to placing the metallic strips and embedding the slots on the ground plane. To avoid these complexities, different shaped microstrip feed such as Y-shaped feed,[17] monopole feed with DR loaded,[18] meandered-line feed,[19] flag-shaped feed,[20] and truncated rectangular patch feed[21] are introduced to generate CP radiation fields. Other technique such as edge feed of microstrip line[22,23] is also utilized to generate CP characteristics in the DR. Here, microstrip feed line and geometry of DR is unmodified to provide broadband CP characteristics. Different microstrip feeding structure approaches for circular polarization are shown in Figure 4. Detailed outcomes of numerous methods of excitation of microstrip line feed are reported in Table 1.[11-23]

From the above excitation of different conventional microstrip line, the DR is directly placed on top of the

TABLE 2 Evolution matrices of coaxial feed with unmodified DRAs[24-34]

References	DR shape	$\epsilon_{r,dr}$	Imp BW (GHz)	AR BW (GHz)	G (dB)	η (%)	Modes	CP mechanism
24	Elli.	12	~8.85-10.2	~9.3-9.7	NM	NM	NM	Feed with DR
25	Hexa.	59	3-3.475	~3–3.4	—	—	$HE_{11\delta}$	Feed with DR
26	Rect.	9.3	~4-4.4	3.96-4.56	4	NM	TE^{y}_{112}	Metallic strips
27	Rect.	9.2	~2.9-3.6	~3.1-3.55	~5	NM	TE^{y}_{111}	Metallic strips
28	Cyli.	11.53	~3.25-3.61	~3.4-3.53	7.7	NM	$HE_{11\delta}$	Metallic strips
29	Trai.	10	7.27-7.44 8.45-9.4	7.38-7.48 8.6-8.77	2.15, 3.69	90	NM	Metallic strips
30	Rect.	10	6.95-8.68	7.47-8.25	5	NA	$TE^{x}_{\delta 13}, TE^{y}_{\delta 13}$	Metallic strips
31	Hemi.	3, 1, 5	~2.9-4.1	~3.3-3.45	NM	NM	NM	Metallic strips
32	Cyli.	10	2.37-2.64	2.38-2.51	1.12	76	$HEM^{x}_{12\delta+1} HEM^{y}_{12\delta+1}$	Metallic loading
33	Cyli.	6.85	2.33-2.54	2.35-2.50	0.7	80	$TM_{01\delta}$	Loop on ground
34	Rect.	36	~2.25-2.7	2.39-2.48	NM	NM	NM	DR loaded patch

Note: "~": estimated from graph; AR BW, axial ratio bandwidth; Cyli., cylindrical; Elli., elliptical; G, gain; H. Cyli., half cylindrical; Hemi., hemispherical; Hexa., hexagonal; Imp BW, impedance bandwidth; NM, not mentioned; Rect., rectangular; Squa., square; Tech., technique; Trai., triangular; $\epsilon_{r,dr}$, dielectric constant of DR; η, efficiency.

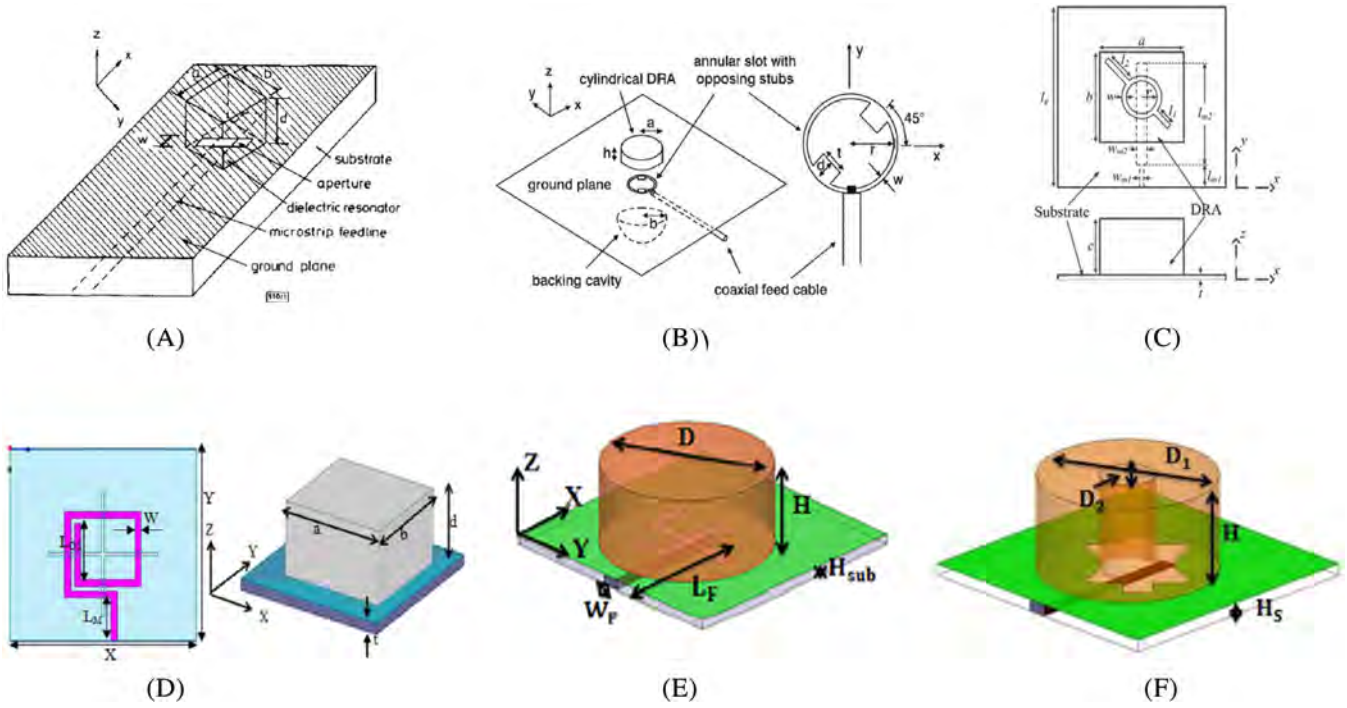

FIGURE 6 Different aperture coupling feeding structure approaches for circular polarization (A) Rectangular slot,[35] (B) Annular slot,[38] (C) Modified Slot,[40] (D) Cross slot with spiral feed,[52] (E) Swastik slot,[61] (F) Modified square slot[64]

microstrip transmission line which is printed on the top layer of the substrate. Due to this, it provides less fabrication complexity but it creates air gap between the DR and the substrate of the antenna, causing a shift in the resonance frequency of the DRA. The other drawback of this feed is that the transmission feeding line is not isolated from the DR that can affect the radiation performance of the DRA by creating spurious radiation in the feeding network. In order to avoid the air gap, the conformal microstrip feed is used. Here, the DR is directly placed on substrate and the microstrip transmission line is attached to the DR walls.

TABLE 3 Evolution matrices of aperture coupled feed with unmodified dielectric resonator antennas (DRAs)[35-64]

References	DR shape	$\epsilon_{r,dr}$	Imp BW (GHz)	AR BW (GHz)	G (dB)	η (%)	Modes	CP mechanism
35	Rect.	40	~5.21-5.65	NM	NM	NM	TE^{x}_{111},TE^{y}_{111}	Rect. slot
36	Rect.	10.8	~14.6-14.8	14.35-14.8	NM	NM	NM	Rect. slot
37	Trape.	9.4	2.88-4.04	3.11-3.86	8.4	NM	NM	Rect. slot
38	Cyli.	9.5	~1.85- > 2	~1.87-1.93	4.5	NM	NM	Annular slot
39	Cyli.	10.2	5.78-7.16	6.22-7.28	6.09	95	$HEM_{11\delta}$	Annular slot
40	Rect.	12	1.58-1.73 2.39-2.76	1.61-1.57 2.65-2.75	5.4 5.8	NM	TE_{111},TE_{113}	Annular slot
41	Cyli.	9.5	~4.5-5.6	~4.75-4.83	4	NM	NM	Annular slot + parasitic patch
42	Hemi.	9.5	~3.25-3.7	~3.45-3.57	NM	NM	NM	Rect. slot + parasitic patch
43	Rect.	9.8	3.46-3.58, 5.1-5.9	3.46-3.54 5.18-5.34	5.4 5.7	93.7 96.2	NM	Trai. slot + parasitic strip
44	Cyli.	9.8	~4.3-6.2	~5.6-5.8	3.5	NM	$HEM_{11\delta}$	Cross slot
45	Hemi.	10.3	~2.7-3.3	~3.05-3.2	4	NM	NM	Cross slot
46	Rect.	12	1.8-2.07 2.57-2.92	1.97-2.03 2.97-2.89	4.7 5.6	NM	NM	Cross slot
47	Rect.	13 3.5	10-13	10.4-11.44	11.1	NM	TE_{119},$TE_{11,\ 11}$, $TE_{11,\ 13}$	Cross slot
48	Rect	10	2.19-3.53	2.19-3.63	4.69	90	NM	Cross slot
49	Rect.	45, 2.2	10.25-13	10.5-13	15.5	NM	TE_{111}	Cross slot
50	Rect.	11	2.19-2.92	2.25-2.88	5	95	TE^{x}_{113},TE^{y}_{113}	Mod. cross slot
51	Rect.	20.5	1.21-1.36, 1.5-1.637	1.19-1.38, 1.474-1.63	5.4 4.3	NM	TE_{111},TE_{113}	Mod. cross slot+ plus sh. feed
52	Rect.	9.8	2.65-3.65	3.12-3.74	4.5	93	TE^{x}_{111},TE^{y}_{111}	Cross slot + spiral feed
53	Rect.	9.8	2.93-3.61	3.19-3.60	5.07	83.55	$TE_{11\delta}$	Plus sh. slot + ring feed
54	Cyli.	9.8	2.72-3.15, 3.4-4.15	3.4-3.45, 3.71-3.94	5.96	NM	$HE^{x}_{11\delta}$,$HE^{y}_{11\delta}$	Squa ring slot + T-sh. feed
55	Cyli.	6.15	~8.3-10.6	~9.25-10.3	3.2	90	$TM_{01\delta}$	L-sh. slot + inclined feed
56	Cyli.	9.8	2.36-3.22 5.0-5.34	2.68-3.04 5.12-5.34	~6.8 ~1	NM	$HE^{x}_{11\delta}$,$HE^{y}_{11\delta}$	Mod. squa slot + Y-sh. feed
57	Cyli.	9.8	2.48-2.98 4.66-5.88	4.9-5.35	~5.5 ~ 6	NM	$HEM_{11\delta}$,$HEM_{12\delta}$	Invert pentagon slot + mod. Feed
58	Squa.	9.8	5.15-5.65	5.2-5.63	4.75	95	TE^{x}_{211},TE^{y}_{121}	Mod. squa. Ring slot + Tsh. feed
59	Cyli.	79	2.35-2.51	2.39-2.48	2.7	NM	NM	Ring slot
60	Cyli.	79	~1.3-1.45	NM	8.2	NM	$HEM_{11\delta}$	C-sh. slot
61	Cyli.	9.8	2.2-2.45 3.0-3.55	2.32-2.45 3.0-3.32	3 5.1	90	$HE^{x}_{11\delta}$,$HE^{y}_{11\delta}$	Swastik slot
62	Cyli.	10	2.32-2.55	2.39-2.51	2.58	89.2	$TM_{01\delta}TM_{01\delta+1}$	Mod. alford loop slot
63	Cyli.	9.8	2.42-2.90 4.9-5.98	2.55-2.72 4.9-5.68	5.5 6.1	NM	$HE_{11\delta}$,$HE_{12\delta}$ $HE_{12\delta\text{ - like}}$	Mod. cir. Slot
64	Cyli.	8	2.8-3.58 5.5-5.92	2.8-3.2 5.85-6.0	~4.5 5.3	NM	$HEM_{11\delta}$,$HEM_{12\delta}$	Mod. squa. Slot

Note: "~": estimated from graph; AR BW, axial ratio bandwidth; Cyli., cylindrical; Elli., elliptical; G, gain; H. Cyli., half cylindrical; Hemi., hemispherical; Hexa., hexagonal; Imp BW, impedance bandwidth; Mod., modified; NM, not mentioned; Rect., rectangular; Squa., square; Sh., shaped; Tech., technique; Trai., triangular; Trape., trapezoidal; $\epsilon_{r,dr}$, dielectric constant of DR; η, efficiency.

Coaxial probe feed

In this feed techniques, the DR is excited through proper placement of coaxial probe. Initially, the researchers have investigated CP characteristics by adjusting the proper placement of coaxial probe feed to different geometries of DR like elliptical structure[24] and hexagonal structure.[25] Later, several novel techniques are used by the researchers to realize the performance of CP. Starting from single fed RDRA excited by outer square spiral conducting strip,[26] single fed RDRA excited by an open half

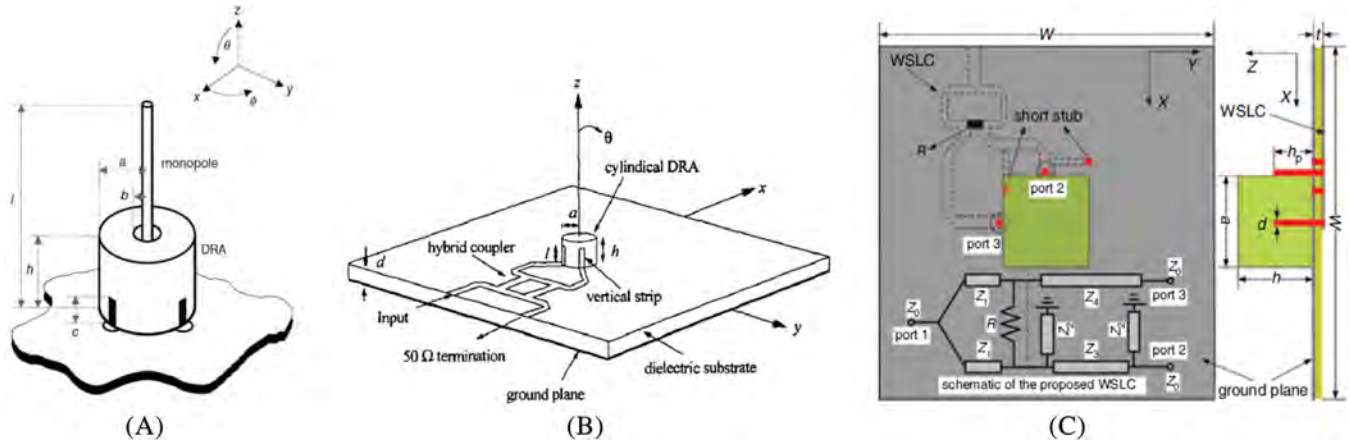

FIGURE 7 Multipoint feed and microwave power divider (A) Multipoint feed,[66] (B) Microwave hybrid coupler,[70] (C) Microwave Wilkinson Splitter[73]

TABLE 4 Evolution matrices of DRA excited by multi-point feed power divider circuit[65-76]

References	DR shape	$\epsilon_{r,dr}$	Imp BW (GHz)	AR BW (GHz)	G (dB)	η (%)	Modes	Excitation techniques
Multi-point feeding technique								
65	Cyli.	37	∼4.15-4.23	NM	2.9	86	$HE_{11\delta}$	2 probe feed
66	Cyli.	44.8	∼2.1-3.7	NM	4.5	—	$HE_{11\delta}$	2 vertical strips
67	Rect.	10	2.7-3.76	2.6-3.78	6.1	—	TE_{111},TE_{113}	2 vertical strips
68	Cyli.	38	∼3.07-3.24	3.07-3.16	4.5	96.3	$HE_{11\delta}$,$TM_{01\delta}$	Modified feed
69	Rect.	10	∼2.02-2.8	2.23-2.78	6.18	—	TE^{x}_{111},TE^{y}_{111}	Modified feed
Microwave Hybrid Coupler								
70	Cyli.	9.5	5-5.7	5.1-6.2	4.5	NM	NM	90° HC
71	Cyli.	9.5	1.75-2.48	1.65-2.14	4.95	80	NM	2 pair 90° HC
72	Cyli.	10	1.08-1.82	∼1-2	3.75	70	NM	180° HC
Microwave Wilkinson Splitter								
73	Rect.	8.9	5-8.15	5.4-8.15	6.4	NM	NM	WS + 90° PS
74	Rect.	12	4.58-7.7	4.78-7.3	6	NM	NM	WS + 90° PS
75	Cyli.	10	4.5-7.65	4.63-7.55	6.4	NM	NM	WS + 90° PS
76	Cyli.	9.8	1.4-2.12	1.69-1.85	10.1	NM	NM	WS + 2 conf. Strips

Note: "∼": estimated from graph; AR BW, axial ratio bandwidth; Conf., conformal; Cyli., cylindrical; G, gain; H. Cyli., half cylindrical; HC, hybrid coupler; Imp BW, impedance bandwidth; NM, not mentioned; PS, phase shifter; Rect., rectangular; Tech., technique; Trai., triangular; Trape., trapezoidal; WS, Wilkinson splitter; $\epsilon_{r,dr}$, dielectric constant of DR; η, efficiency.

loop consisting of three metallic strips,[27] single fed CDRA excited by an external metallic strip around the DR like helix structure,[28] triangular DRA with dual facet spiral loop on both side of the DR walls[29] and RDRA with a new H-shaped conformal metallic strip[30] are implemented to generate orthogonal modes resulting in CP radiation waves. Moreover, the researchers investigated CP by utilizing three-layer hemispherical DRA fed by a conformal strip with parasitic patch.[31] Here, the adjustment of conformal strip and inserted parasitic patch inside the different layer are used to generate CP radiation waves. Consequently, CDRA with a top-loaded modified Alford loop[32] and novel CDRA consisting of light emitting diode (LED), glass DR and four open-ended logarithmic spiral slots in the ground plane[33] and DR loaded patch[34] are investigated for demonstrating CP characteristics. Different coaxial probe feeding structure approaches for circular polarization are illustrated in Figure 5. The detailed outcomes of numerous methods of excitation of coaxial probe feed for the sake of generating of CP radiation fields are reported in Table 2.[24-34]

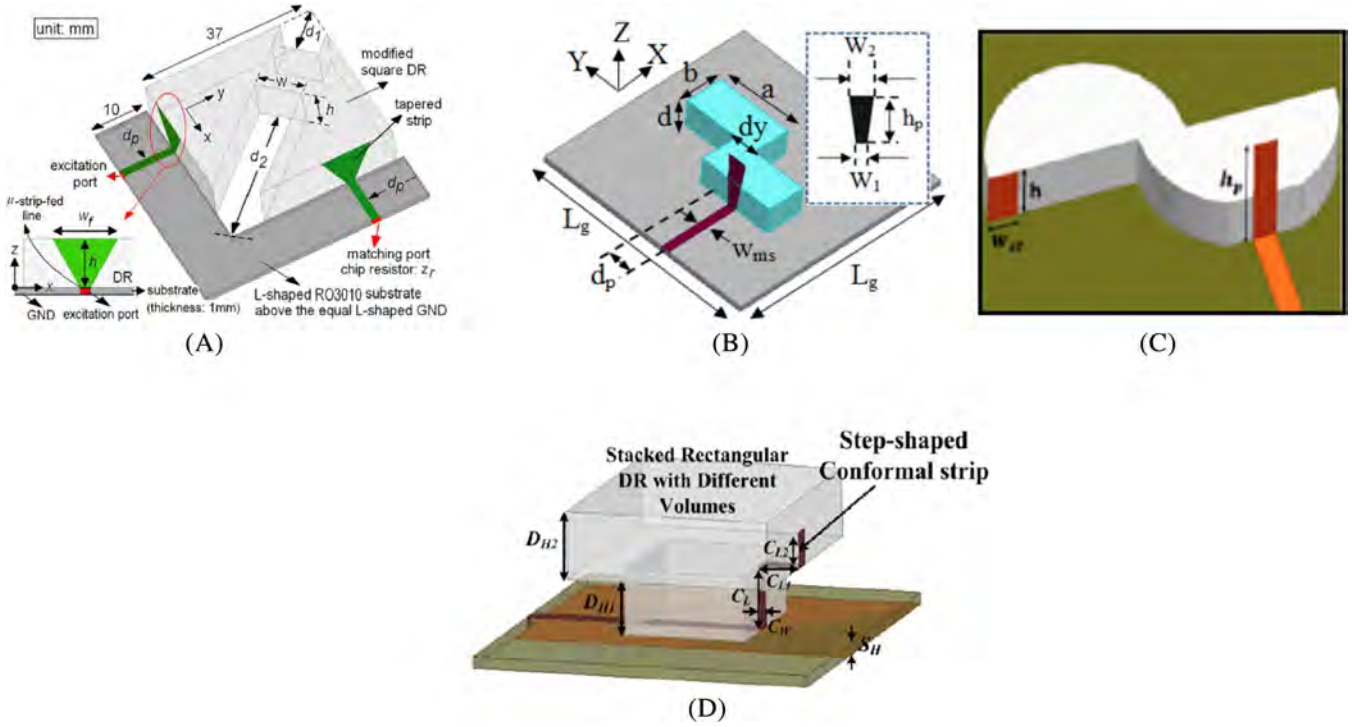

FIGURE 8 Different dielectric resonator shapes with microstrip feed approaches for circular polarization (A) Modified RDRA with inclined slits,[78] (B) Stair shaped DR,[79] (C) Modified DR with metallic strips,[80] (D) Stacked rectangular DR[81]

From the above literature, the excitation of coaxial probe feed that is, probe is penetrating DR, it provides high coupling to the DR that results in high radiation efficiency. The main drawback of this feed is that a small hole needs to be drilled in the DRA. The dimensions of the drilled hole need to be perfectly matched with the dimensions of the probe that is, length and diameter, otherwise the effective dielectric constant of the DR will be affected causing a shift in the resonance frequency of the DRA. As a result, the overall fabrication process is more expensive and complex. To avoid the fabrication complexity, the coaxial probe is connected adjacently to the DR, but it exhibits less coupling to the DRA as compared to penetrating coaxial probe feeding.

Aperture coupled feed

To enhance the performance of polarization fields, aperture slot coupling excitation techniques is widely used in many structure of the DRA. The working methodology behind this excitation is that an electromagnetic signal is coupled to DR through different shapes of aperture and radiates into the free space. Other point of interest is to reduces the radiation from feeding circuit. In this literature survey, various geometrical shaped of coupling aperture have been used for producing the CP radiation waves. Initially, simple rectangular slot[35] has been used to excite the signal and produce orthogonal nearly degenerate modes to generate the CP radiation waves. Later, a 45° rotated rectangular DR with respect to aperture slot[36] and 45° rotated slot with respect to rectangular DR[37] are introduced to achieve CP fields. In order to improve the impedance matching with better CP, the researchers have presented modified annular slots like annular slot with opposing stubs,[38] annular slot with open stub,[39] annular slot with two linear slot arms,[40] which excited electromagnetic signal to the DR. In addition, different slots with parasitic patch[41-43] are also responsible to generate orthogonal modes. In spite of single slot techniques, the antenna designers introduced the dual slot aperture also known as cross slot[44-50] on the ground plane and modifying cross slot with various shaped of feed like plus shaped[51] and spiral shaped.[52] These techniques do not only generate CP characteristics, but also provide better coupling between the feed and DR. In addition, the combinations of different geometrical shaped slots with different shape of feed[53-58] are utilized to produce CP characteristics with proper impedance matching. Other slot techniques such as ring slot,[59] C-shaped slot,[60] swastik slot,[61] modified Alford loop slot,[62] modified circular slot,[63] and modified square slot[64] are responsible for generating CP response. Different aperture coupling feeding structure approaches for circular polarization are shown in Figure 6. Detailed results are reported in terms

TABLE 5 Evolution matrices of microstrip line feed with modified DR[77-81]

References	DR shape	$\epsilon_{r,dr}$	Imp BW (GHz)	AR BW (GHz)	G (dB)	η (%)	Modes	CP mechanism
77	Mod Rect.	10.2	3.4-5.95	3.4-5.75	6.6	89	NM	Mod. rect. DR + loops
78	Mod Squa.	10	3.08-5.18	2.86-4.43	6	9.8	NM	Inc. slits loaded DR
79	Stair Rect.	10.2	4.6-6.7	5.2-6.5	5.7	90	$TE^{x}_{121}\,TE^{y}_{211}$	Stair sh. DR
80	Inverted Sigmoid	12.8	5.51-7.46 11.8-12.37	6.08-7.43 11.84-12.2	4.85, 6.38	80	$HEM_{11\delta}\text{HEM}_{22\delta}$	Meta. strip + mod. DR
81	Stacked Rect.	9.8	2.17-3.81	2.21-2.48	5.80	89.4	$TE^{x}_{\delta 11}, TE^{y}_{1\delta 1}$,	Stacked rect DR

Note: AR BW, axial ratio bandwidth; G, gain; Imp BW, impedance bandwidth; Inc., inclined; Mod., modified; NM, not mentioned; Rect., rectangular; Sh., shaped; Squa., square; $\epsilon_{r,\,dr}$, dielectric constant of DR; η, efficiency.

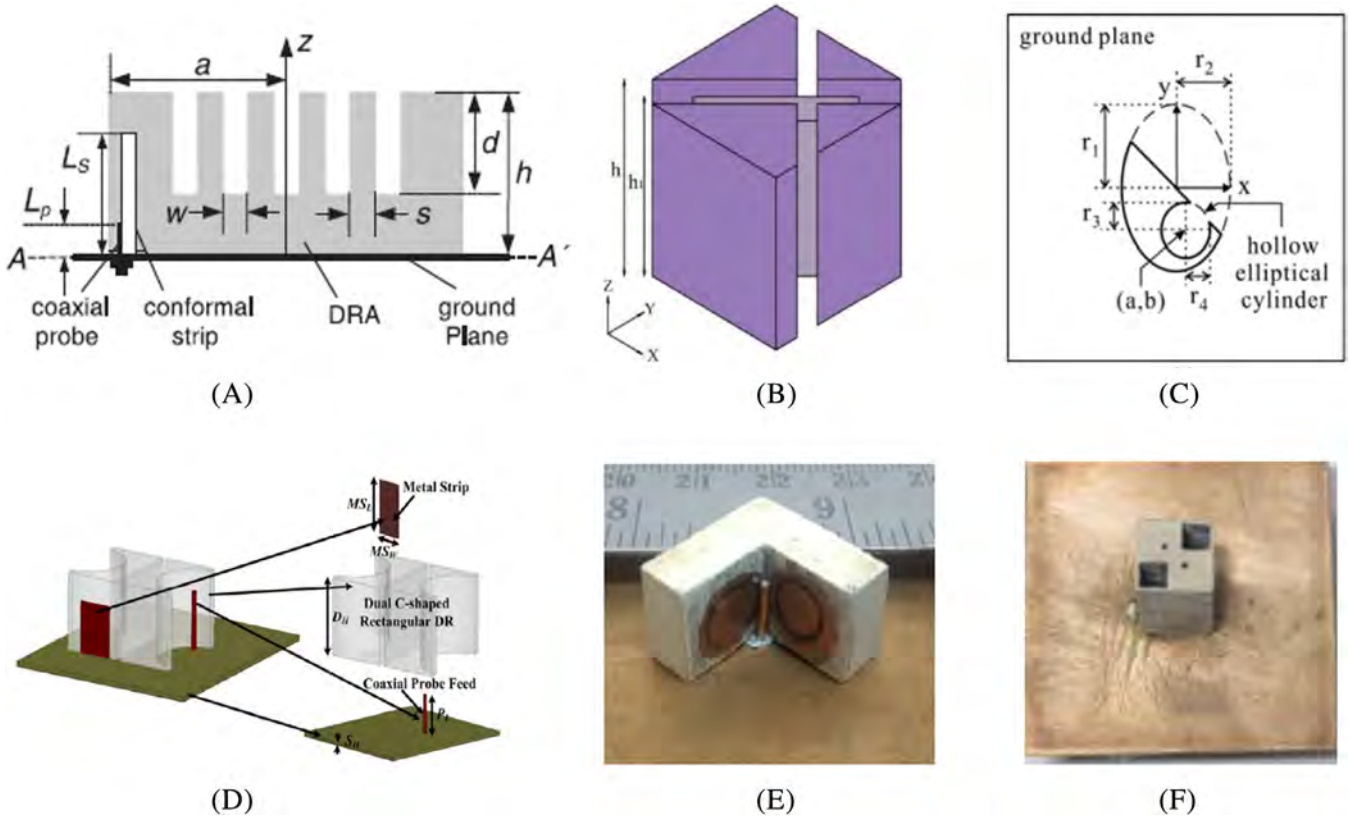

FIGURE 9 Different dielectric resonator shapes with coaxial probe feed approaches for circular polarization (A) Comb shaped DR,[84] (B) Modified DR,[87] (C) Semi-eccentric annular DR[89] (D) Dual C-shaped DR,[92] (E) V-shaped DR with circular metallic patch,[93] (F) Perturbation of square slots on DR[94]

of impedance bandwidth, AR bandwidth, gain, efficiency, modes and CP mechanism of aperture coupled feed in Table 3.[35-64]

From the above study, the aperture coupled feed avoids direct electromagnetic interaction between the feed line and DRA. Due to this feeding technique, the spurious radiation from the feeding network can be reduced and it enhanced the polarization purity of the DRA. In addition, it provides less fabrication complexity.

3.1.2 | Multi-point feed and microwave power divider

To obtain wider bandwidth with circular polarized fields, multipoint feeding technique is used as an excitation of DRA. To generate CP radiation, two conditions must be satisfied: (a) generation of orthogonal modes within the DR (b) phase quadrature relationship between orthogonal modes. Single point feeding technique is used to generate orthogonal modes with narrow band CP, which

TABLE 6 Performance of dielectric resonator antennas (DRAs) of coaxial probe feed with modified DR[82-94]

References	DR shape	$\epsilon_{r,dr}$	Imp BW (GHz)	AR BW (GHz)	G (dB)	η (%)	Modes	CP mechanism
82	Mod Cyli.	12	∼2.39-3.35	2.54-2.81	12	NM	TM_{011},$TM_{21\delta}$	Circular sector
83	Mod Cyli.	9.8	4.65-7.6	5.43-6.34	5.8	>80	$TM_{v,1,\delta}$, $TM_{2v,1,\delta}$,	Circular sector
84	Mod Cyli.	10	∼4.3-4.85	∼4.68-4.8	3.5	NM	NM	Comb sh. DR
85	Qua. Cyli.	13.3	2.18-2.54	2.21-2.29	∼4.8	NM	$TM_{01\delta}$,$TM_{41\delta}$	Qua. cyli. sh. DR
86	Mod Rect.	15	2.30-2.94	2.39-2.57	1.6	NM	TM_{011}	Slot on DR
87	Mod Rect.	10	5.13-5.37	5.15-5.36	2.13	NM	NM	Inclined slits+ mod. DR
88	Mod Rect.	6.6	2.08-2.98	2.31-2.72	5.5	70	$TE^{x}_{\delta 11}$,$TE^{y}_{1\delta 1}$	Truncated corner DR
89	Mod. Elli.	10	9.41-12.62	10.3-10.9	4.78	NM	NM	Semi-eccentric annular DR
90	Mod Rect.	15	3.08-3.94	3.16-4.08	1.48	98	NM	Slot on DR+ PS
91	Mod Rect.	10	6.5-12.18	8.31-9.24 10.1-11.6	4.86 4.91	NM	NM	Chamfered corner and PS
92	C-shaped	9.8	3.22-4.36	3.25-3.77	5.2	88	$TE^{x}_{\delta 11}$,$TE^{y}_{1\delta 1}$	Dual C-sh. rect. + metallic strip
93	V-Shaped	10	7.85-10.1	8.35-8.7	4.8	94	NM	V-sh. DR + cir. Metallic patches
94	Mod Rect.	10.2	4.7-7.7, 4.6-7	5.7-6.4 4.7-6	NM	NM	TE_{111},TE_{113}	Perturbation of square slots

Note: "∼", estimated from graph; AR BW, axial ratio bandwidth; Cyli., cylindrical; Elli., elliptical; G, gain; Imp BW, impedance bandwidth; Mod., modified; MS, metallic strip; NM, not mentioned; PS, parasitic strip; Qua., quadrature; Rect., rectangular; Sh., shaped; $\epsilon_{r,\,dr}$, dielectric constant of DR; η, efficiency.

mostly depends on shapes of the DR. With the trivial characteristics of multi-point feeding mechanism, CP is generated and considered to be independent from the shape of the DR. However, the drawback of the multi-point feed arrangement is the requirement of additional circuit area for designing this type of feeding network. Thus, there would be a limitation on regards to the size when considering miniaturized system. To further undergo in this area, the researchers have investigated the scope of multi-point feed techniques[65-69] and power divider that is, Hybrid coupler[70-72] and Wilkinson splitter[73-76] to realize the CP characteristics while achieving trade-offs. Microwave power divider circuits are used to divide the input power into two equal magnitude and 90° phase delay in between, which lead to generate orthogonal modes producing CP radiation waves. In addition, the hybrid coupler excitation method is used with microstrip line to enable direct integration with monolithic microwave integration circuits (MMICs). Another microwave power divider called Wilkinson splitter with wideband 90° phase shifter excitation demonstrates circular polarization with wideband characteristics. The multi-point feeds and microwave power dividers are shown in Figure 7. Detailed results are reported in terms of −10 dB impedance bandwidth, 3-dB AR bandwidth, realized gain, antenna efficiency, modes and excitation techniques in Table 4.[65-76]

3.2 | Modified DR shapes with excitation of feed

Another way to generate CP characteristics is by modifying the shape of DR with excitation of different feeding mechanism. This leads in generating of the orthogonal modes needed for CP excitation. This section highlights the rapid development of CPDRA using modified DR structure utilizing different feeding mechanism such as microstrip line feed, coaxial probe feed and aperture coupled feed.[77-103]

3.2.1 | Research on modified DR shapes with microstrip feed

The research on creating CP utilizing modified DR that is excited by single microstrip feed and conducting loops on ground plane started with configuration of rectangular ring DR housed inside the substrate.[77] In this structure, several conducting loops are printed on the ground plane to achieve a wider CP bandwidth. Later, the researchers introduced a novel square DR loaded with two unequal inclined slits to obtain CP characteristics.[78] Here, the key parameters such as position of the excitation, matching lines and the impedance of the chip resistor have been carefully optimized to enhance the CP performance. A novel CPDRA technique that is, implementation of two

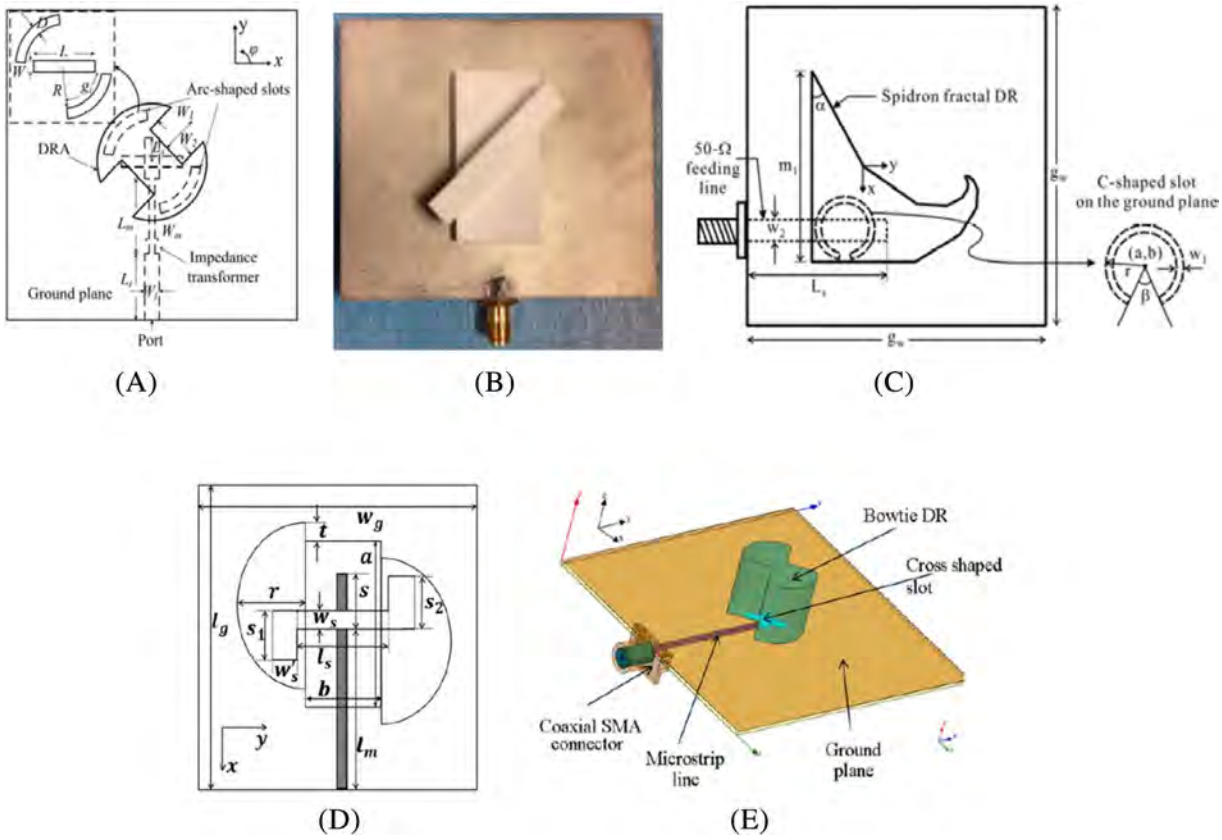

FIGURE 10 Different dielectric resonator shapes with aperture coupled feed approaches for circular polarization (A) Arc shaped slot with modified DR,[97] (B) Rectangular slot with rotated DR,[98] (C) C-shaped slot with spidron fractal,[100] (D) Stair shaped slot with modified DR,[102] (E) Cross shape slot with bowtie DR[103]

rectangular DR, which are joined together to form a stair-shaped DRA is investigated for wideband CP response.[79] In order to generate multiband CP response, the inverted sigmoid shaped DRA with metallic strip is proposed.[80] Other technique to generate CP radiation is stacked rectangular DR[81] consists of stacked DR with different volume, combined of stepped-shaped conformal metallic strip with microstrip line feed and partial ground plane. But, this structure leads to increase the height of the overall antenna size, which may not be suitable for particular application, where thickness is restricted. Different modified DR shapes with microstrip feed approaches for circular polarization are shown in Figure 8 and their detailed results are reported in Table 5.[77-81]

3.2.2 | Research on modified DR shapes with coaxial feed

In this section, the authors have reported different techniques behind CP radiation by using modified DR shapes with excited by coaxial probe feed. The researchers have investigated the work on CP radiation by modifying the DR shaped like cylindrical shaped into circular sector,[82,83] comb shaped,[84] and quadrature shaped.[85] Additionally, rectangular shaped DR are modified by removing the inclined slots on the side walls of the DR,[86,87] truncated corner of the DR[88] and hollow elliptical into semi-elliptical shaped DR,[89] which have been investigated to realize CP characteristics. Due to use of slots on each side of DR, it generates wide axial bandwidth with omnidirectional radiation pattern.[82-94]

Moreover, the implementation of parasitic strips/metallic strips on the side of the modified DR such as modified rectangular DR with parasitic strips,[90] chamfered corner of rectangular DR with parasitic strip,[91] dual C-shaped with metallic strip,[92] and V-shaped with metallic strip[93] is utilized to generate orthogonal modes. Another technique to generate wideband CP response is by the implementation of perturbation in the form of square slots along the diagonal of RDRA.[94] The key parameter of this design is the existence of slots, which excite two orthogonal modes with same magnitude and quadrature in phase. The different DR shapes with coaxial probe feed approaches for circular polarization are

TABLE 7 Evaluation matrices of aperture feed with modified dielectric resonator (DR)[95-103]

References	DR shape	$\epsilon_{r,dr}$	Imp BW (GHz)	AR BW (GHz)	G (dB)	η (%)	Modes	CP mechanism
95	Stair Rect.	12	7.56-10.95	9.4-10.45	NM	NM	NM	Rect. slot + rotated stair DR
96	Fan blade	12.8	3.29-3.92 4.52-6.25	3.29-3.76 4.55-4.92	4.2	NM	TE_{111},TE_{211}	Rect slot + fan blade shape DR
97	Mod. Cyli.	9.8	4.6-5.99 8.54-9.55	4.78-5.6 8.94-9.4	4.3 5.8	NM	HE_{111},$HE_{11\delta}$	Rect slot + two notch cyli. DR
98	Stack Rect.	9.8	4.9-6.7	5-6	4.5	NM	TE_{111},TE_{113}	Rect. slot + rotated DR
99	Cyli.	10	7.1-8.4	8-8.32	5.92	NM	$HEM_{11\delta}$	Rect slot + mod. Gnd. plane
100	Fractal	10	4.32-6.30	5.13-5.76	3.16	NM	NM	C-slot + spidron fractal DR
101	Stair Rect.	9.8	3.84-8.14	4.15-6.63	3.9	97	TE^{x}_{111},TE^{y}_{111}	Open slot gnd. + stair DR
102	Rect. + Split Cyli.	12.8	4.1-6.81	4.40-6.67	>1.5	>80	TE^{x}_{111},TE^{y}_{111}	Stair Slot and Rect. + half Cyli. DRs
103	Bowtie	10.2	6.75-10.53	7.8-8.4	5.8	NM	NM	Cross slot + bowtie DR

Note: AR BW, axial ratio bandwidth; Cyli., cylindrical; G, gain; gnd., ground; Imp BW, impedance bandwidth; Mod., modified; NM, not mentioned; Rect., rectangular; $\epsilon_{r,\,dr}$, dielectric constant of DR; η, efficiency.

shown in Figure 9. Their obtained characteristics are given in Table 6.

3.2.3 | Research on modified DR shapes with aperture feed

This section explores the modified DR with excitation of aperture coupled slot feed to producing the CP characteristics. Rectangular slot with different shaped of DRs such as rotated stair DR,[95] fan blade shaped DR,[96] cylindrical DR with implementation of dual notch[97] which are truncated at 45° and 225°, two rectangular stacked DRs with rotation angle of 46° relative to the adjacent bottom layer[98] and symmetric tapered sheets on either side of the feed line[99] are used to generate orthogonal modes in DR which in turn produces CP waves.[95-103]

To achieve wide impedance bandwidth with wide axial bandwidth, the implementation of fractal geometry concept plays crucial role. The intuition behind the usage of fractal shape in DRA is that, the number of fractal iteration is directly proportional to the surface to volume ratio of DR. It is also inversely proportional to Q-factor. Therefore, decreasing Q-factor leads to increase in impedance bandwidth. By utilizing this concept, researchers have presented spidron fractal DR with C-shaped slot in the ground plane[100] to achieve wide impedance bandwidth and axial bandwidth. Other novel technique to generate wideband CP response is by the implementation of stair-shaped DR with an open ended slot ground plane.[101] In spite of these, other techniques such as stair shaped slot with combined rectangular DR and two half slits cylindrical DR,[102] and cross slot with bowtie DR are responsible to generate CP characteristics.[103] Different DR shapes with aperture coupled feed approaches for CP are shown in Figure 10. Their detailed results are reported in Table 7.

From Tables 1 to 7, a detailed state-of-the-art development of CPDRA is studied and reported. Here, authors have highlighted the rapid development of CPDRA using various mechanism such as feeding techniques (single point feed and multi-point feed power divider that is, Hybrid coupler and Wilkinson splitter) and modified DR shaped in terms of different excitation techniques such as microstrip line, coaxial probe and aperture coupled feed. This survey article is helpful to the DRA researcher to explore and investigate various techniques on realizing CP for DRA. In spite of literature survey, the authors have presented a compact CP rectangular DRA to generate CP radiation waves. Finally, the potential applications found in the open literature are discussed in Section 5.

4 | PROPOSED STRUCTURE

4.1 | A compact circularly polarized modified rectangular DRA

The proposed antenna comprises of rectangular DR shape placed on a ground plane and excited by a 50-Ω coaxial probe feed. To achieve CP characteristics, two unequal vertical slits are etched on both corner of

rectangular DR. The electric field orientation at different phases that is, 0°, 90°, 180°, and 270° are analyzed and reported. The proposed antenna offers simulated bandwidth of 47.5% (2.34-3.80 GHz), measured impedance bandwidth of 50.8% (2.26-3.80) and simulated axial bandwidth is 13% (3.29-3.75 GHz) respectively. Other antenna parameter such as peak realized gain and radiation efficiency are 7.7 dBi and 98% within operating frequency bands respectively.

4.2 | Antenna geometry

The schematic diagram of the proposed DRA is shown in Figure 11. It consists of modified rectangular DR shape with permittivity ($\epsilon_{r,\ [dra]}$) of 9.8 and loss tangent (tan δ) of 0.002, placed on the perfect electric conductor (PEC) ground plane. It is fed to DR by a coaxial probe with flat metallic strip to have better impedance matching. This proposed design is an extension of a rectangular DRA. The dimensions of RDRA are calculated by using the following curve fitting equations.[88]

$$f_{GHz} = \frac{15F}{\pi w_{\mathrm{dra(cm)}}\sqrt{\epsilon_{r,\mathrm{dra}}}} \tag{5}$$

where, F denotes as normalized frequency of the RDRA that is determined by the following Equation (6):

$$F = X_0 + X_1\left(\frac{W_{\mathrm{dra}}}{2H_{\mathrm{dra}}}\right)^1 + X_2\left(\frac{W_{\mathrm{dra}}}{2H_{\mathrm{dra}}}\right)^2 \tag{6}$$

where,

$$X_0 = 2.57\text{-}0.8\left(\frac{L_{\mathrm{dra}}}{2H_{\mathrm{dra}}}\right)^1 + 0.42\left(\frac{L_{\mathrm{dra}}}{2H_{\mathrm{dra}}}\right)^2 - 0.05\left(\frac{L_{\mathrm{dra}}}{2H_{\mathrm{dra}}}\right)^3$$

$$X_1 = 2.71\left(\frac{L_{\mathrm{dra}}}{2H_{\mathrm{dra}}}\right)^{-0.282}$$

$$X_2 = 0.16$$

where f_{GHz} is the resonant frequency at 2.4 GHz. $\epsilon_{r,dra}$ is permittivity of DR and W_{dra}, L_{dra} and H_{dra} are the width, length and height of the DR in cm respectively.

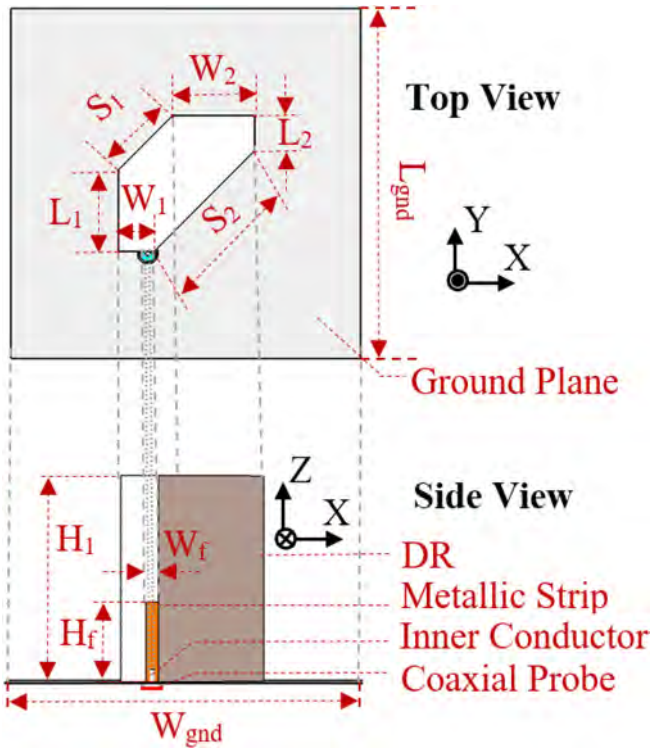

FIGURE 11 The schematic diagram of proposed DRA. (Optimized dimensions: $L_{gnd} = W_{gnd} = 60$, $H_1 = 29.5$, $L_1 = W_2 = 13.8$, $W_1 = L_2 = 6$, $S_1 = 13$, $S_2 = 24$, $H_f = 12.8$, $W_f = 2$. All dimensions are in mm)

4.3 | Antenna design procedure

The evolution of the proposed modified RDRA as shown in Figure 12, is carried out to achieve wide impedance bandwidth and AR bandwidth. The simulation results of input reflection coefficient vs frequency

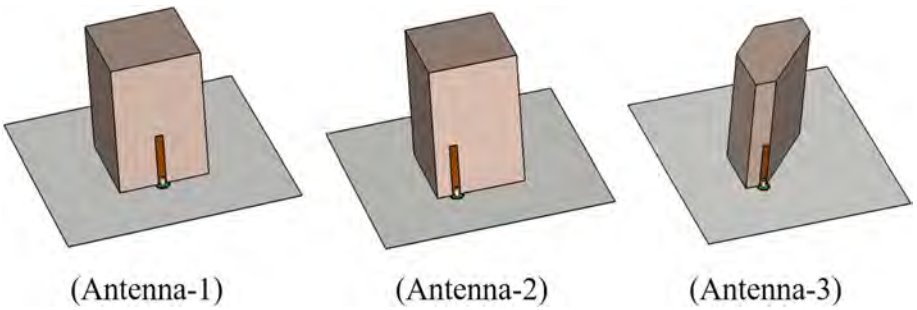

FIGURE 12 Evolution of proposed modified RDRA

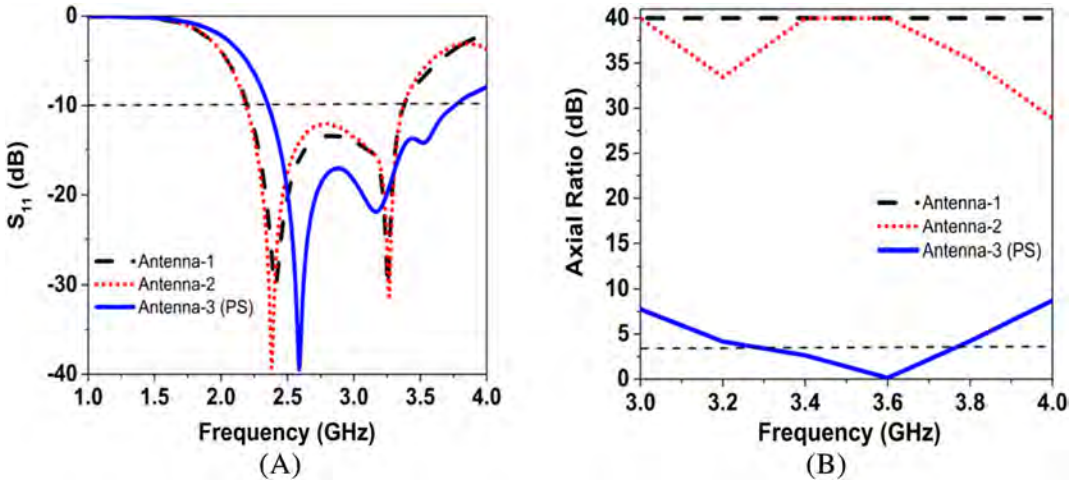

FIGURE 13 Simulated results of proposed modified RDRA (A) S_{11} vs frequency (B) axial ratio vs frequency

TABLE 8 Comparison results of evolution steps of proposed DRA

Antenna steps	Path length (mm)	Volume/surface	Res. frequency (GHz)	Imp. bandwidth (GHz)	AR bandwidth (GHz)
Antenna-1	92	4.14	2.4	2.19-3.39	NA
Antenna-2	92	4.14	2.4	2.18-3.38	NA
Antenna-3 (PS)	76.6	3.57	2.6	2.34–3.80	3.29-3.75

Abbreviations: AR, axial ratio; Imp., impedance; PS, proposed structure; Res., resonant.

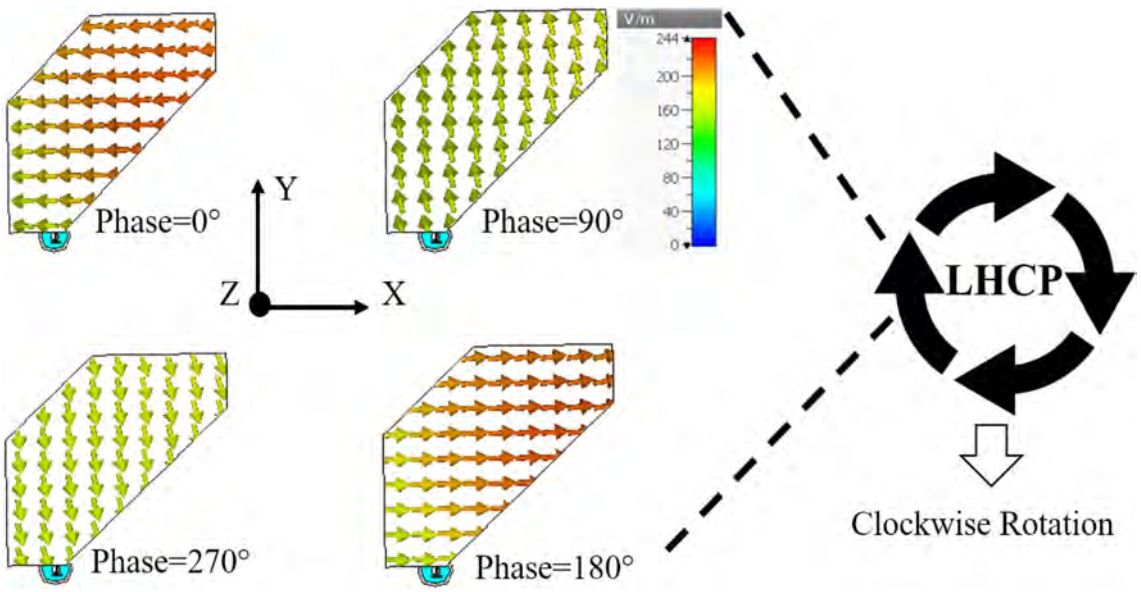

FIGURE 14 Top view of simulated electric field distribution of the proposed DRA for different phases at 3.6 GHz

and axial ratio bandwidth vs frequency of each modification that is, antenna-1 to antenna-3 (PS) are illustrated in Figure 13. Here, all dimensions are constant except the DR shape.

4.3.1 | Antenna-1

In this proposed antenna, the rectangular DR shape is excited at the center by using a coaxial probe. The coaxial

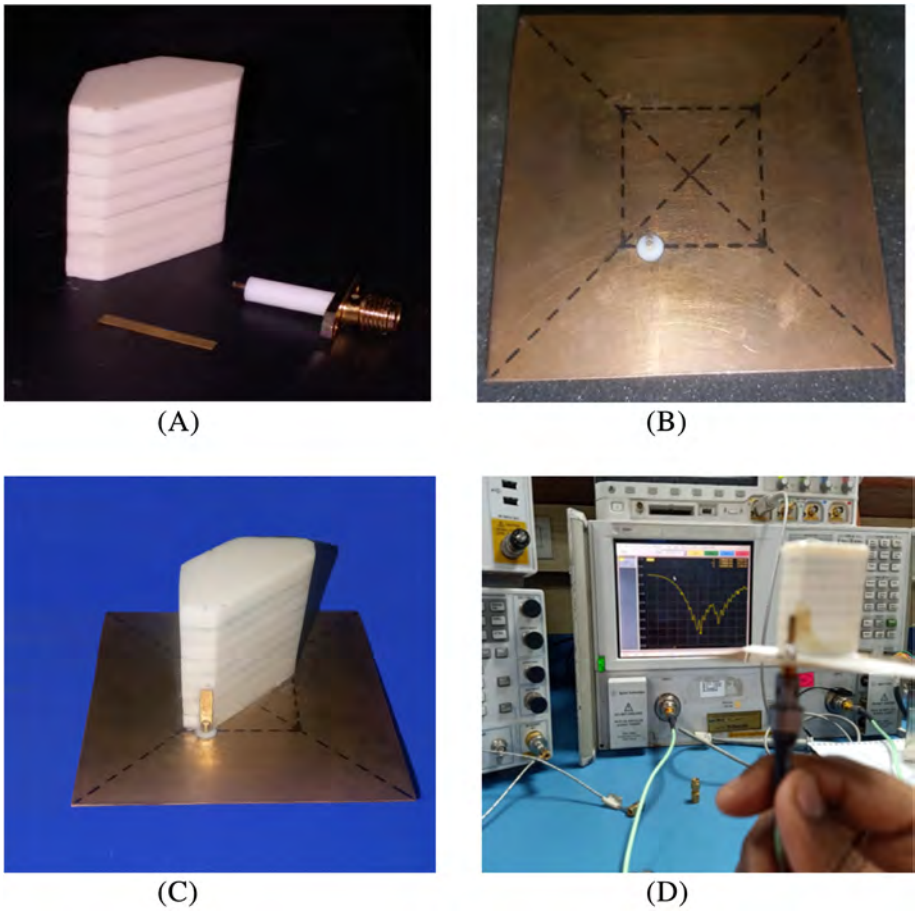

FIGURE 15 Fabricated prototype along with the experimental setup of the proposed DRA (A) Fabricated DR, metallic strip, coaxial probe (B) Ground plane along with coaxial probe (C) 3D view of the proposed antenna (D) S_{11} measurement using VNA

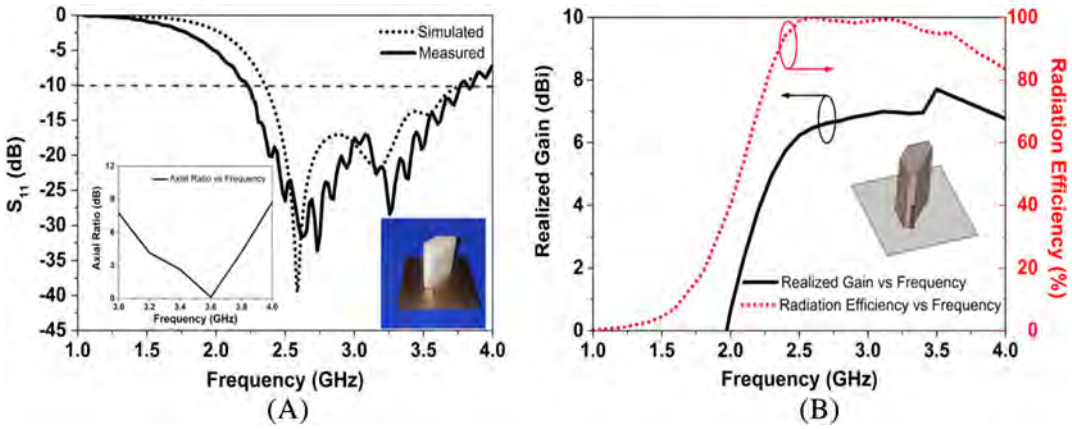

FIGURE 16 Outcomes of the proposed DRA (A) S_{11} and axial ratio vs frequency (B) Realized gain and radiation efficiency vs frequency

probe feed acts like a short magnetic dipole in the z-direction which excites $TE^{x}_{\delta 11}$ mode inside the RDRA. Here, the antenna starts to radiate electromagnetic energy into free space, but it is unable to generate orthogonal modes that can be seen in Figure 13B. In addition, the inner conductor of coaxial probe is connected with a flat metallic strip which is placed adjacent to the rectangular DRA, whose length, width and position can be adjusted to improve the impedance match.

4.3.2 | Antenna-2

Further, to decrease the axial ratio curve from 40 dB line with improvement of impedance matching, the coaxial

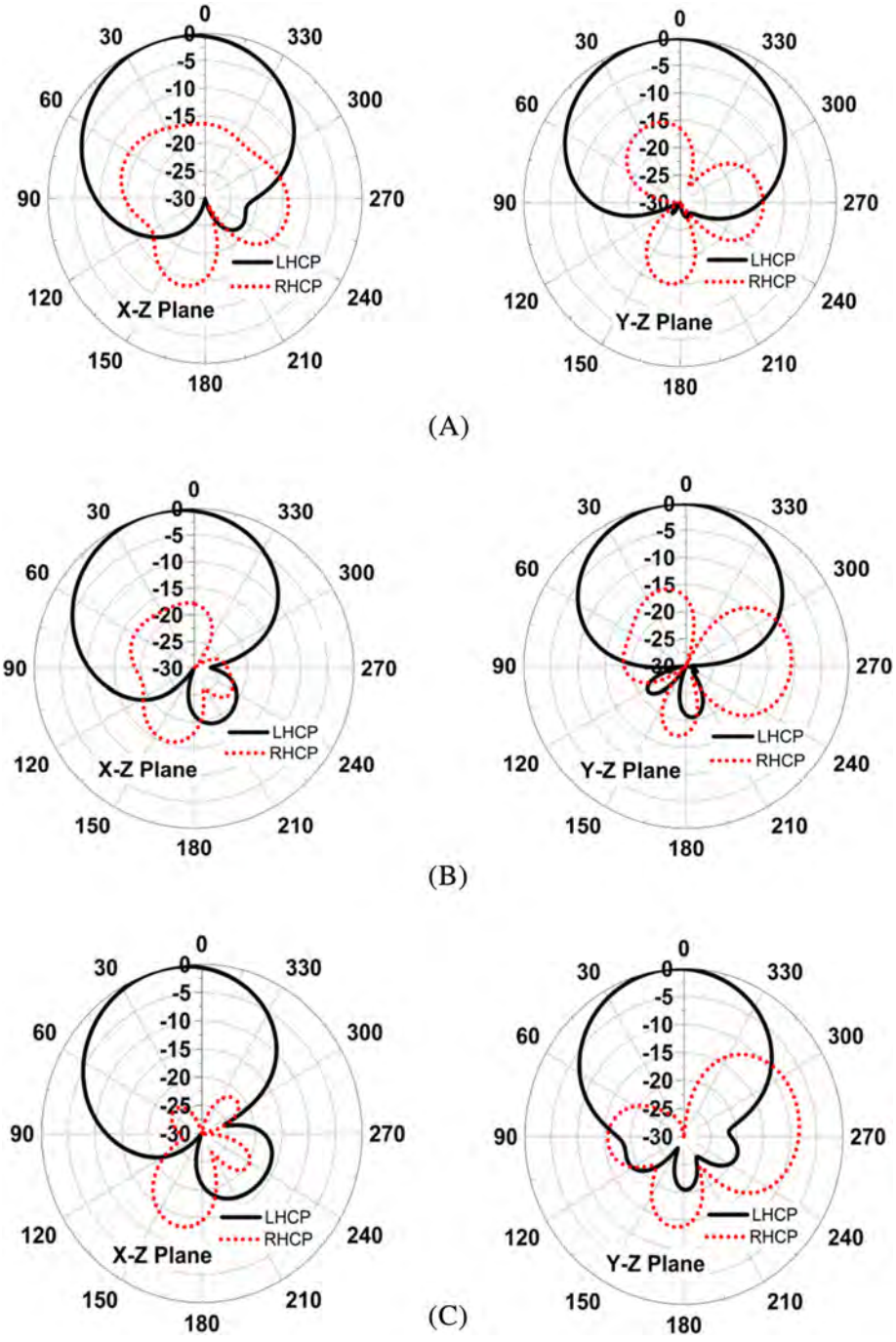

FIGURE 17 Normalized radiation pattern of proposed DRA (A) 3.4 GHz (B) 3.5 GHz (C) 3.6 GHz in X-Z plane and Y-Z plane

probe feed is shifted into left side of the DR (antenna-2). As a result, the axial ratio curve decreases but not up to 3 dB line as shown in Figure 13B. Therefore, it is unable to generate orthogonal modes with equal same magnitudes and orthogonal phase.

4.3.3 | Antenna-3

To generate orthogonal modes, two unequal vertical slits are etched at both corners of rectangular DR (anenna-3). Due to these vertical slits, the peak resonant frequency shifted from 2.4 to 2.6 GHz, because the path length or perimeter of DR is inversely proportional to the resonant frequency.[104] Here, the path length is reduced from 92 mm into 76.6 mm that is, antenna-1 to antenna 3. In addition, the bandwidth of antenna-3 is also increased due to decrease in volume to surface area of DR as shown in following Equation (7).

A general equation linked to the unloaded Q-factor of the antenna geometries[105] is:

TABLE 9 Potential applications in terms of different frequency bands

Band	Technologies/ potential applications	References used
Single-band	Wi-Max/WLAN/Wi-Fi/ Bluetooth/ISM 2400/ GPS	19, 21, 34, 52, 53, 59, 68, 87, 92
	C-band in satellite applications	17, 49, 96, 102
	WBAN (Wireless Body Area Network)	30, PS
Dual-band	WLAN and Wi-MAX	43, 56, 57, 61
	WLAN and radio location applications	97
	Can be used in satellite applications	80, 89, 96
Broadband	Can be used in broadband applications	22,23, 39, 73, 74, 75, 100
Wideband	Can be used in wide-band applications	12, 16, 20, 26, 27, 31, 37, 42, 48, 49, 50, 71, 72, 77, 78, 79, 80, 90, 91, 92, 94, 95, 99, 101, 102

$$Q = 2\omega_0 \frac{\text{Stored Energy}}{\text{Radiated Power}} \propto 2\omega_0 (\varepsilon_r)^p \left(\frac{\text{Volume}}{\text{Surface}}\right)^s \quad with\ p > s \geq 1\ with\ p > s \geq 1 \tag{7}$$

where, ω_0 is the resonant angular frequency. As the resonance frequency is proportional to $\frac{1}{\sqrt{\varepsilon_r}}$, therefore, Equation (7) indicates that the Q-factor is decreased when volume to surface area of DR is reduced and also there is enhancement of bandwidth. The volume to surface area of rectangular DRA (antenna-1 and 2) and proposed DRA (antenna-3) is 4.14 and 3.57 respectively. The comparison results are reported in Table 8.

4.4 | Circular polarization mechanism

In order to generate CP radiation fields, both electric field components should be equal magnitude with odd multiple of 90° phase difference. To verify the orthogonal modes and CP radiation, the electric field distribution is studied at 3.6 GHz as shown in Figure 14. It is observed from the Figure, when phase changes from 0° to 90°, the movement of electric fields also changes according to phase that is, left orientation of electric fields into 90° rotates in clockwise direction which confirm the formation of orthogonal modes in the proposed DRA. Similarly, same behavior is observed when phase changes from 90° to 270°. To identify the left-handed circular polarization (LHCP) or right-handed circular polarization (RHCP) wave, the electric field orientation at four different phases that is, 0°, 90°, 180°, and 270° are analyzed as shown in Figure 14. From this analysis, the rotation of electric field is clockwise direction which implies that the proposed antenna exhibits LHCP radiation.

4.5 | Measurement results and discussion

The prototype is fabricated and shown in Figure 15. Agilent N5247A vector network analyzer (VNA) is used to measure the scattering parameter as shown in Figure 15D. The simulated and measured impedance bandwidth of the proposed antenna are 1.46 GHz (2.34-3.80 GHz) and 1.54 GHz (2.26-3.80), respectively. The simulated AR bandwidths as shown in Figure 16 is found 0.46 GHz (3.29-3.75 GHz) in broadside direction ($\theta = 0°$ and $\phi = 0°$). Due to fabrication tolerance and use of chemical adhesive material in fixing DR and substrate, there is a small discrepancy in between simulated and measured outcomes.

The peak realized gain and radiation efficiency are 7.7 dBi and 98% within operating frequency band as shown in Figure 16B. The simulated far-field normalized radiation pattern of the proposed structure at 3.4, 3.5, and 3.6 GHz in X-Z plane and Y-Z plane are shown in Figure 17A-C. It is observed from normalized radiation pattern that the left-handed CP (LHCP) is having stronger fields than right-handed CP (RHCP) in X-Z plane and Y-Z plane respectively. Hence, the proposed DRA confirm LHCP radiated antenna.

5 | POTENTIAL APPLICATIONS

The utilization of CPDRAs based on implementation of different feeding techniques and modification of DR geometry are quite important from the research point of view, but cognitively it is incomplete without real field of potential applications. By taking the above points, the authors have highlighted the potential applications in terms of frequency band from the instances available in the open literature. The potential applications in terms of different frequency bands are given in Table 9. It gives a brief idea about the progress of research done from applications point of view.

6 | CONCLUSION

In this review article, a complete state-of-the-art is presented to highlight different techniques that essentially helps in achieving circular polarization in DRAs. This article highlights the basic concept of CP mechanism in DRAs and state-of-the-art developments of CPDRAs in terms of single and multi-point feed for unmodified and modified DR geometries considering different types of excitation mechanism such as microstrip line, coaxial probe, and aperture coupled feed. To better understand about CP mechanism, a mathematical modeling is persuaded and correlated with rectangular DRA. To satisfy the trade-offs in existing instances of CPDRAs, authors have proposed a compact modified CP rectangular DRA. The proposed structure provides the simulated and measured −10 dB impedance bandwidth of 1.46 GHz (2.34-3.80 GHz) and 1.54 GHz (2.26-3.80) respectively. The simulated AR bandwidths is found be 0.46 GHz (3.29-3.75 GHz) in broadside direction ($\theta = 0^\circ$ and $\phi = 0^\circ$). Other antenna parameters such as peak realized gain and radiation efficiency are 7.7 dBi and 98% within operating frequency band. From author's point of view, this survey article helpful to the DRA researchers to get complete literature of towards development CP techniques based on various mechanism. During literature survey, authors have tried to their level best to highlights novel contributions of the CPDRA researchers during the periods of last three and half decades, still the authors apologize to the researcher community, if any novel contribution is skipped unknowingly.

DATA AVAILABILITY STATEMENT

Author elects to not share data.

ORCID

Priya Ranjan Meher https://orcid.org/0000-0002-0918-9618
Bikash Ranjan Behera https://orcid.org/0000-0001-8312-4022
Sanjeev Kumar Mishra https://orcid.org/0000-0002-9089-9763
Ayman Abdulhadi Althuwayb https://orcid.org/0000-0001-5160-5016

REFERENCES

1. Mongia RK, Bhartia P. Dielectric resonator antenna-a review and general design relations for resonant frequency and bandwidth. *Int J Microw Millim-Wave Comput Aid Eng*. 1994;4(3):230-247.
2. Soren D, Ghatak R, Mishra RK, Poddar DR. Dielectric resonator antennas: designs and advances. *Prog Electromagn Res B*. 2014;60:195-213.
3. Petosa A, Ittipiboon A. Dielectric resonator antennas: a historical review and the current state of the art. *IEEE Antennas Propag Mag*. 2010;52(5):91-116.
4. Leung KW, Lim EH, Fang XS. Dielectric resonator antennas: from the basic to the aesthetic. *Proc IEEE*. 2012;100(7):2181-2193.
5. Meher PR, Behera BR, Mishra SK. Design and its state-of-the-art of different shaped dielectric resonator antennas at millimeter-wave frequency band. *Int J RF Microwave Comput Aided Eng*. 2020;30(7):1-15.
6. Dash SKK, Khan TDA. Dielectric resonator antennas: an application oriented survey. *Int J RF Microw Comput Aided Eng*. 2017;27(3):1-22.
7. Dash SKK, Khan T, Antar YMM. A state-of-art review on performance improvement of dielectric resonator antennas. *Int J RF Microw Comput Aided Eng*. 2018;28(6):1-19.
8. Richtmyer RD. Dielectric resonators. *J Appl Phys*. 1939;10(6):391-398.
9. Long SA, Mcallister MW, Shen LC. The resonant cylindrical dielectric cavity antenna. *IEEE Trans Antennas Propag*. 1983;31(3):406-412.
10. Balanis CA. *Antenna Theory: Analysis and Design*. New York, NY: Wiley Inter Science; 2009.
11. Lee MT, Luk KM, Yung EKN, Leung KW. Microstrip-line feed circularly polarized cylindrical dielectric resonator antenna. *Micro Opt Tech Lett*. 2000;24(3):206-207.
12. Chowdhury R, Chaudhary RK. Wideband circularly polarized rectangular DRA fed with dual pair of right angled microstrip line. *Int J RF Microwave Comput Aided Eng*. 2016;26(8):713-723.
13. Hslao FR, Chlou TW, Wong KL. Circularly polarized low profile square dielectric resonator antenna with a loading patch. *Micro Opt Tech Lett*. 2001;31(3):157-159.
14. Kumar AVP, Hamsakutty V, Yohannan J, Mathew KT. A strip loaded dielectric resonator antenna for circular polarization. *Micro Opt Tech Lett*. 2006;48(7):1354-1356.
15. Yu C, Ling CW. Frequency-adjustable circular polarized dielectric resonator antenna with slotted ground plane. *Electron Lett*. 2003;39(14):1030-1031.
16. Kumar RN, Chaudhary RK. Wideband circularly polarized hybrid dielectric resonator antenna with bi-directional radiation characteristics for various wireless applications. *Int J RF Microwave Comput Aided Eng*. 2019;29(9):1-10.
17. Li LX, Zhong SS, Xu SQ, Chen MH. Circular polarized ceramics dielectric resonator antenna excited by Y-shaped microstrip. *Microw Comput Aided Eng*. 2009;51(10):2416-2418.
18. Haraz OM, Sebak AR, Denidni TA. A hybrid printed monopole antenna loaded with dielectric resonator for wideband and circular polarization applications. *Int J RF Microwave Comput Aided Eng*. 2012;22(5):588-593.
19. Kumar R, Chaudhary RK. Wideband circularly polarized dielectric resonator antenna coupled with meandered-line inductor for ISM/WLAN applications. *Int J RF Microwave Comput Aided Eng*. 2017;27(7):1-7.
20. Kumari R, Gangwar RK. Circularly polarized rectangular dielectric resonator antenna fed by a flag shape microstrip line for wideband applications. *Micro Opt Tech Lett*. 2018;60(10):2577-2584.
21. Kumari R, Gangwar RK. Wideband circularly polarized square dielectric resonator antenna for WLAN/WiMAX applications. *Int J RF Microwave Comput Aided Eng*. 2019;29(2):1-9.
22. Meher PR, Behera BR, Mishra SK. Broadband circularly polarized cylindrical dielectric resonator antenna for wideband applications. Paper presented at: IEEE International

Conference on Microwave Integrated Circuits, Photonics and Wireless Networks (IMICPW), Tiruchirappalli, India, 2019; 524–528.
23. Meher PR, Behera BR, Mishra SK. Broadband circularly polarized edge feed rectangular dielectric resonator antenna using effective glueless technique. *Micro Opt Tech Lett*. 2020;1-9.
24. Kishk AA. An elliptic dielectric resonator antenna designed for circular polarization with single feed. *Micro Opt Tech Lett*. 2003;37(6):454-456.
25. Hamasakutty V, Kumar AVP, Yohannan J, Mathew KT. Coaxial fed hexagonal dielectric resonator antenna for circular polarization. *Micro Opt Tech Lett*. 2006;48(3):581-582.
26. Sulaiman MI, Khamas SK. A single fed rectangular dielectric resonator antenna with a wideband circular polarization. *IEEE Antennas Wirel Propag Lett*. 2010;9:615-618.
27. Sulaiman MI, Khamas SK. A single fed wideband circularly polarized dielectric resonator antenna using concentric half-loops. *IEEE Antennas Wirel Propag Lett*. 2011;10:1305-1308.
28. Motevasselian A, Ellgardt A, Jonsson BLG. A circularly polarized cylindrical dielectric resonator antenna using a helical exciter. *IEEE Trans Antenna Propag*. 2013;61(3):1439-1443.
29. Dash SKK, Khan T, Kanaujia BK. Circularly polarized dual facet spiral fed compact triangular dielectric resonator antenna for sensing applications. *IEEE Sensor Lett*. 2017;2(3):1-4.
30. Illahi U, Iqbal J, Silaiman MI, et al. Design of new circularly polarized werable dielectric resonator antenna for off-body communication in WBAN applications. *IEEE Access*. 2019;7: 573-582.
31. Kakade AB, Kumbhar MS. Wideband circularly polarized conformal strip fed three-layer hemispherical dielectric resonator antenna with parasitic patch. *Micro Opt Tech Lett*. 2014; 56(1):72-77.
32. Li WW, Leung KW. Omnidirectional circularly polarized dielectric resonator antenna with top-loaded Alford loop for diversity design. *IEEE Trans Antenna Propag*. 2013;61(8): 4246-4256.
33. Yang N, Leung KW, Wu N. Omnidirectional circularly polarized dielectric resonator antenna with logarithmic spiral slots in the ground. *IEEE Trans Antenna Propag*. 2017;65(2): 839-844.
34. Tsai CL, Deng SM, Chen T, Liu LW. Circularly polarized dielectric resonator-loaded circular microstrip patch antennas for WLAN 2.4 GHz applications. *Micro Opt Tech Lett*. 2009;51 (6):1470-1473.
35. Oliver MB, Antar YMM, Mongia RK, Ittipiboon A. Circularly polarized rectangular dielectric resonator antenna. *Electron Lett*. 1995;31(6):418-419.
36. Esselle KP. Circularly polarized higher-order rectangular dielectric resonator antenna. *Electron Lett*. 1996;32(3):150-151.
37. Pan Y, Leung KW. Wideband circularly polarized trapezoidal dielectric resonator antenna. *IEEE Antennas Wirel Propag Lett*. 2010;9:588-591.
38. Leung KW, Mok SK. Circularly polarized dielectric resonator antenna excited by perturbed annular slot with backing cavity. *Electron Lett*. 2001;37(15):934-936.
39. Zhang Z, Wang XM, Jiao YC, Weng ZB. Broadband circularly polarized dielectric resonator antenna with annular slot excitation. *Prog Electromagn Res C*. 2013;40:105-117.
40. Meng Z, Pan J. A simple dual-band circularly polarized rectangular dielectric resonator antenna. *Prog Electromagn Res C*. 2015;53:57-63.
41. Leung KW, Wong WC, Ng HK. Circularly polarized slot-coupled dielectric resonator antenna with a parasitic patch. *IEEE Antennas Wirel Propag Lett*. 2002;1:57-59.
42. Leung KW, Ng HK. The slot-coupled hemispherical dielectric resonator antenna with a parasitic patch: application to the circularly polarized antenna and wideband antenna. *IEEE Trans Antenna Propag*. 2005;53(5):1762-1769.
43. Gupta A, Gangwar RK. Dual-band circularly polarized aperture coupled rectangular dielectric resonator antenna for wireless applications. *IEEE Access*. 2018;6:11388-11396.
44. Almpanis G, Fumeaux C, Vahldieck R. Offset cross-slot coupled dielectric resonator antenna for circular polarization. *IEEE Microwave Wireless Compon Lett*. 2006;16(8):461-463.
45. Li B, Leung KW. On the circularly polarized hemi-ellipsoidal dielectric resonator antenna. *Micro Opt Tech Lett*. 2006;48(9): 1763-1766.
46. Zou M, Pan J, Nie ZP. Investigation of a cross-slot coupled dual band circularly polarized hybrid dielectric resonator antenna. *Prog Electromagn Res C*. 2014;53:187-195.
47. Khalil AAAY, Khamas S. Higher order mode circularly polarized two-layer rectangular dielectric resonator antenna. *IEEE Antennas Wirel Propag Lett*. 2018;17(6):1114-1117.
48. Yang MD, Pan YM, Yang WJ. A single fed wideband circularly polarized dielectric resonator antenna. *IEEE Antennas Wirel Propag Lett*. 2018;17(8):1515-1518.
49. Sun WJ, Yang WW, Chen JX. Design a wideband circularly polarized stacked dielectric resonator antenna. *IEEE Trans Antenna Propag*. 2019;67(1):591-595.
50. Zou Meng PJ. Wideband hybrid circularly polarized rectangular dielectric resonator antenna excited by modified cross slot. *Electron Lett*. 2014;50(16):1123-1125.
51. Wang XC, Sun L, Lu XL, Liang S, Lu WZ. Single feed dual band circularly polarized dielectric resonator antenna for CNSS applications. *IEEE Trans Antenna Propag*. 2017;65(8): 4283-4287.
52. Kumari R, Gangwar RK. Circularly polarized rectangular dielectric resonator antenna fed by a cross aperture coupled spiral microstrip line. *Int J RF Microwave Comput Aided Eng*. 2017;28(2):1-7.
53. Kumar R, Chaudhary RK. Circularly polarized rectangular DRA coupled through orthogonal slot excited with microstrip circular ring feeding structure for Wi-MAX applications. *Int J RF Microwave Comput Aided Eng*. 2017;28(1):1-7.
54. Kumari R, Gangwar RK. Circularly polarized cylindrical dielectric resonator antenna excited by square ring slot with a T-shaped microstrip line. *Microw Opt Tech Lett*. 2017;59(10):2507-2514.
55. Mishra NK, Das S, Vishwakarma DK. Low profile circularly polarized cylindrical dielectric resonator antenna coupled by L-shaped resonator slot. *Microw Opt Tech Lett*. 2017;59(5):996-1000.
56. Sharma A, Das G, Gangwar RK. Dual-band circularly polarized hybrid antenna for WLAN/Ai-MAX applications. *Microw Opt Tech Lett*. 2017;59(10):2450-2457.
57. Sharma A, Das G, Gangwar RK. Dual-band dual polarized hybrid aperture cylindrical dielectric resonator antenna for wireless applications. *Int J RF Microw Comput Aided Eng*. 2017;27(5):1-9.
58. Kumari R, Gangwar RK. Circularly polarized slot coupled square dielectric resonator antenna for WLAN applications. *Microw Opt Tech Lett*. 2018;60(11):2787-2794.
59. Lin CC, Sun JS. Circularly polarized dielectric resonator antenna fed by off-centred microstrip line for 2.4 GHz ISM

band applications. *IEEE Antennas Wirel Propag Lett*. 2014;14: 947-949.
60. Huang CY, Kuo JS. Frequency adjustable circularly polarized dielectric resonator antenna. *Microw Opt Tech Lett*. 2002;34 (3):211-213.
61. Sharma A, Tripathi DK, Das G, Gangwar RK. Novel asymmetrical swastik-shaped aperture coupled cylindrical dielectric resonator antenna with dual-band and dual-sense circular polarization characteristics. *Microw Opt Tech Lett*. 2019;61(2): 405-411.
62. Guo L, Leung KW. Compact uni-lateral circularly polarized dielectric resonator antenna. *IEEE Trans Antenna Propag*. 2018;66(2):668-674.
63. Sharma A, Das G, Gangwar RK. Dual-band circularly polarized modified circular aperature loaded cylindrical dielectric resonator antenna for wireless applications. *Microw Opt Tech Lett*. 2017;59(7):1562-1570.
64. Pathak D, Sharma SK, Kushwah VS. Investigation on circularly polarized ring dielectric resonator antenna for dual-band wireless applications. *Prog Electromagn Res M*. 2017;62: 123-130.
65. Drossos G, Wu Z, Davis LE. Circularly polarized cylindrical dielectric resonator antenna. *Electron Lett*. 1996;32(4):281-283.
66. Gray D, Watanabe T. Three orthogonal polarization DRA-monopole ensemble. *Electron Lett*. 2003;39(10):766-767.
67. Li B, Hao CX, Sheng XQ. A dual-mode quadrature fed wideband circularly polarized dielectric resonator antenna. *IEEE Antennas Wirel Propag Lett*. 2009;8:1036-1038.
68. Hady LK, Kishk AA, Kajfer D. Dual-band compact DRA with circular and monopole like linear polarizations as a concept for GPS and WLAN applications. *IEEE Antennas Wirel Propag Lett*. 2009;57(9):2591-2598.
69. Lim EH, Leung KW, Fang XS. The compact circularly polarized hollow rectangular dielectric resonator antenna an underlaid quadrature coupler. *IEEE Antennas Wirel Propag Lett*. 2011;59(1):288-293.
70. Leung KW, Wong WC, Luk KM, Yung EKN. Circular polarized dielectric resonator antenna excited by dual conformal strips. *Electron Lett*. 2000;36(6):484-486.
71. Khoo KWK, Guo YX, Ong LC. Wideband circularly polarized dielectric resonator antenna. *IEEE Antennas Wirel Propag Lett*. 2007;55(7):1929-1932.
72. Massie G, Caillet M, Clenet M, Antar YMM. A new wideband circularly polarized hybrid dielectric resonator antenna. *IEEE Antennas Wirel Propag Lett*. 2010;9:347-350.
73. Han RC, Zhong SS, Liu J. Broadband circularly polarized dielectric resonator antenna fed by wideband switched line coupler. *Electron Lett*. 2014;50(10):725-726.
74. Han RC, Zhong SS, Liu J. Design of broadband circularly polarized dielectric resonator antenna using improved feed network. *Microw Opt Tech Lett*. 2014;56(9):2191-2195.
75. Sun RY. Bandwidth enhancement of circularly polarized dielectric resonator antenna. *ETRI J*. 2015;35(1):26-31.
76. Kumari R, Gangwar RK. Circularly polarized cylindrical dielectric resonator antenna excited by dual conformal strips along with modified wilkinson power divider for high gain application. *Microw Opt Tech Lett*. 2017;59(4):908-913.
77. Mohsen K, Rahim MKA, Kishk AA. Planar wideband circularly polarized antenna design with rectangular ring dielectric resonator and plastic printed loops. *IEEE Antennas Wirel Propag Lett*. 2012;11:905-908.
78. Khalily M, Kamarudin MR, Jamaluddin MH. A novel square dielectric resonator antenna with two unequal inclined slits for wideband circular polarization. *IEEE Antennas Wirel Propag Lett*. 2013;12:1256-1259.
79. Fakhte S, Oraizi H, Karimian R, Fakhte R. A new wideband circularly polarized stair-shaped dielectric resonator antenna. *IEEE Antennas Wirel Propag Lett*. 2015;63(4):1828-1832.
80. Varshney G, Gotra S, Pandey VS, Yaduvanshi RS. Inverted-sigmoid shaped multi-band dielectric resonator antenna with dual band circular polarization. *IEEE Trans Antenna Propag*. 2018;66(4):2067-2072.
81. Kumar R, Chaudhary RK. Stacked rectangular dielectric resonator antenna with different volumes for wideband circular polarization coupled with step-shaped conformal strip. *Int J RF Microwave Comput Aided Eng*. 2019;29(6):1-8.
82. Tam MTK, Murch RD. Circularly polarized circular sector dielectric resonator antenna. *IEEE Trans Antenna Propag*. 2000;48(1):126-128.
83. Chowdhury R, Chaudhary RK. Investigation on different forms of circular sectored-dielectric resonator antenna for improvement in circular polarization performance. *IEEE Trans Antenna Propag*. 2018;66(10):5596-5601.
84. Chu LCY, Guha D, Antar YMM. Comb-shaped circularly polarized dielectric resonator antenna. *Electron Lett*. 2006;42 (14):785-787.
85. Bezerra JWO, Sousa DG, Junqueira CCM, Silva MAS, Barroso GC, Sombra ASB. Circularly polarized quarter cylindrical shaped dielectric resonator antenna using a single probe feed. *Microw Opt Tech Lett*. 2015;57(3):722-726.
86. Pan YM, Leung KW, Lu K. Omnidirectional linearly and circularly polarized rectangular dielectric resonator antennas. *IEEE Trans Antenna Propag*. 2012;60(2):751-759.
87. Khalily MK, Kamarudin MR, Mokayef M, Jamaluddin MH. Omnidirectional circularly polarized dielectric resonator antenna for 5.2 GHz WLAN applications. *IEEE Antennas Wirel Propag Lett*. 2014;13:443-446.
88. Chen Z, Wong H. Liquid dielectric resonator antenna with circular polarization reconfigurability. *IEEE Trans Antenna Propag*. 2018;66(1):444-449.
89. Lee JM, Kim SJ, Kwon G, et al. Circularly polarized semi-eccentric annular dielectric resonator antenna for X-band applications. *IEEE Antennas Wirel Propag Lett*. 2015;14:1810-1813.
90. Pan YM, Leung KW. Wideband omnidirectional circularly polarized dielectric resonator antenna with parasitic strips. *IEEE Trans Antenna Propag*. 2012;60(6):2992-2997.
91. Abedian M, Rahim SKA, Danesh S, Jamaluddin MH. A compact wideband circularly polarized dielectric resonator antenna. *Electron Lett*. 2016;53(1):5-6.
92. Kumar R, Nasimuddin N, Chaudhary RK. A new dual C-shaped rectangular dielectric resonator based antenna for wideband circularly polarized radiation. *Int J RF Microwave Comput Aided Eng*. 2019;29(6):1-12.
93. Singhwall SS, Kanaujia BK, Singh A, Kishor J. Circularly polarized V-shaped dielectric resonator antenna. *Int J RF Microwave Comput Aided Eng*. 2019;29(9):1-10.
94. Patel P, Mukherjee B, Mukherjee J. Wideband circularly polarized rectangular dielectric resonator antenna using square shaped slots. *IEEE Antennas Wirel Propag Lett*. 2015; 15:1309-1312.
95. Chair R, Yang SLS, Kishk AA, Lee KFL, Luk KM. Aperture fed wideband circularly polarized rectangular stair shaped

dielectric resonator antenna. *IEEE Trans Antenna Propag*. 2006;54(4):1350-1352.
96. Varshney G, Pandey VS, Yaduvanshi RS. Dual-band fan-blade shaped circularly polarized dielectric resonator antenna. *IET Microw Antenna Propag*. 2017;11(12):1868-1871.
97. Zhou YD, Jiao YC, Weng ZB, Ni T. A novel single-fed wide dual band circularly polarized dielectric resonator antenna. *IEEE Antennas Wirel Propag Lett*. 2015;15:930-933.
98. Wang KX, Wong H. A circularly polarized antenna by using rotated-stair dielectric resonator. *IEEE Antennas Wirel Propag Lett*. 2015;14:787-790.
99. Dash SKK, Khan T, Kanaujia BK. Wideband circularly polarized cylindrical dielectric resonator antenna for X-band applications. *Int J RF Microwave Comput Aided Eng*. 2017;59(10):2463-2468.
100. Altaf A, Yang Y, Lee KY, Hwang HC. Circularly polarized spidron fractal dielectric resonator antenna. *IEEE Antennas Wirel Propag Lett*. 2015;14:1806-1809.
101. Lu L, Jiao YC, Zhang H, Wang R, Tian L. Wideband circularly polarized antenna with stait-shaped dielectric resonator and open-ended slot ground. *IEEE Antennas Wirel Propag Lett*. 2016;15:1755-1758.
102. Varshney G, Pandey VS, Yaduvanshi RS, Kumar L. Wideband circularly polarized dielectric resonator antenna with stair-shaped slot excitation. *IEEE Trans Antennas Propag*. 2017;65(3):1380-1380, 1383.
103. Chauthaiwale P, Chaudhary RK, Srivastava KV. Circularly polarized bowtie shaped dielectric resonator antenna excited with asymmetric cross slot. *Micro Opt Tech Lett*. 2015;57(7):1723-17274.
104. Meher PR, Behera BR, Mishra SK. Design of different shaped DRAs for 60 GHz millimeter-wave applications. *IEEE Ind Conf Antennas Propog Ind*. 2018;1-4.
105. Babik GB, Nallo CD, Faraonc A. Multimode dielectric resonator antenna of very high permittivity. *IEEE Antenna Propag*. 2004;2:1383-1386.

AUTHOR BIOGRAPHIES

Priya Ranjan Meher received M. Tech Degree with specialization in communication System Department of Electronics and Communication Engineering from GIET University, Gunupur, Odisha, India in 2015. He is currently pursuing Ph. D. in RF and Microwaves, Department of Electronics and Telecommunication Engineering with International Institute of Information Technology Bhubaneswar, Odisha, India. Mr. Meher has authored and co-authored in more than 13 papers, in reputed conferences and journals. His research interests are Broadband circularly polarized dielectric resonator antenna, Wireless body area network antenna (WBAN), RF-energy harvesting systems and nanophotonics. Mr. Meher is a student member of IEEE.

Bikash Ranjan Behera received M. E. Degree with specialization in Wireless Communication, Department of Electronics and Communication Engineering from Birla Institute of Technology Mesra, Ranchi, Jharkhand, India in 2016. He is currently pursuing Ph.D. in RF and Microwaves, Department of Electronics and Telecommunication Engineering with International Institute of Information Technology Bhubaneswar, Odisha, India. In 2017, he is the recipient of Young Scientist Award at URSI-RCRS'17, Tirupati, India. He has authored and co-authored in more than 25 papers in reputed conferences and journals. His research interests are RF energy harvesting systems, metamaterials-inspired antenna designing, and the study of EM based optimization techniques. Mr. Behera is a student member of IEEE.

Dr Sanjeev Kumar Mishra (M'13-SM'16) received his Ph.D. degree in Electrical Engineering from IIT Bombay, Mumbai, India in 2012. He served as a Research Associate (2004-2005), Scientist B (2005-2007) at ICRS, Visiting Faculty (2012-2013), and Assistant Professor (2014-July 2016) at IIST, ISRO, DoS, Government of India. He is currently working as an Assistant Professor in the Department of Electronics and Telecommunication Engineering at IIIT Bhubaneswar. His research interest includes RF and Microwave Circuits and System Design, Planar Antennas Design, RADAR Systems, Wireless Communication, RF and Microwave Measurements. He has published more than 75 papers in IEEE, PIER, MOTL, IJACSP, JMPCE, IJRFMCAE international and IETE, CSIR-IJRSP, CSIR IJAP national journals and conferences. His research work has been cited in more than 600 journal papers. He has written a book and 2 patents in the field of antennas. He received Young Scientist International Travel Support from DST and CSIR, Government of India to attend the international conferences. He is also a reviewer of IEEE, IETE, PIERS, Elsevier and IET journals. He has also reviewed a number of IEEE, PIERS international and national conference papers.

Dr Ayman Althuwayb received the B.Sc. degree (Hons.) in electrical engineering (electronics and communications) from Jouf University, Saudi Arabia, in 2011, the M.Sc. degree in electrical engineering from California State University,

Fullerton, California, in 2015, and the Ph.D. degree in electrical engineering from Southern Methodist University, Dallas, Texas, in 2018. He is currently an Assistant Professor with the department of electrical engineering at Jouf University, Kingdom of Saudi Arabia. His current research interests include antenna design and propagation, microwaves and millimeter-waves, wireless power transfer, ultrawideband and multiband antennas, filters and other.

How to cite this article: Meher PR, Behera BR, Mishra SK, Althuwayb AA. A chronological review of circularly polarized dielectric resonator antenna: Design and developments. *Int J RF Microw Comput Aided Eng*. 2021;31:e22589. https://doi.org/10.1002/mmce.22589